

A COMPARATIVE ANALYSIS OF SHALLOW WATER MAPPING TOOLS

by

Geoffrey S. Cleveland

A Thesis

Submitted to the

Graduate Faculty

of

George Mason University

in Partial Fulfillment of

The Requirements for the Degree

of

Master of Science

Geoinformatics and Geospatial Intelligence

Committee:

_____	Dr. Arie Croitoru, Thesis Director
_____	Dr. Anthony Stefanidis, Committee Member
_____	Dr. Ruixin Yang, Committee Member
_____	Dr. Anthony Stefanidis, Department Chair
_____	Dr. Donna M. Fox, Associate Dean, Office of Student Affairs & Special Programs, College of Science
_____	Dr. Peggy Agouris, Dean, College of Science

Date: \_\_\_\_\_ Fall Semester 2015  
George Mason University  
Fairfax, VA

A Comparative Analysis of Shallow Water Mapping Tools

A Thesis submitted in partial fulfillment of the requirements for the degree of Master of  
Geoinformatics and Geospatial Intelligence at George Mason University

by

Geoffrey S. Cleveland  
Bachelor of Science  
George Mason University, 2015

Director: Arie Croitoru, Professor  
Department of Geography and GeoInformation Science

Fall Semester 2015  
George Mason University  
Fairfax, VA

## **DEDICATION**

This is dedicated to my loving woman Nicole, who supports me in work, education and life. Additionally, this dedication is to the cats four Sonja, Gucci, Dior and Dell who managed to spend countless hours next to me pondering why I would sit in front of a computer only paying minimal attention to them.

## **ACKNOWLEDGEMENTS**

I would like to thank the many friends that I have worked with at George Mason University, the Professors, and the knowledgeable peers at the Army Geospatial Center (AGC) and the supporters that have made the development and writing of this thesis possible. Particular thanks go out to the AGC Water Resources Group for their historic and current knowledge on the topics this thesis covers.

## TABLE OF CONTENTS

	Page
List of Tables .....	vi
List of Figures .....	vii
Abstract .....	ix
Chapter 1: Introduction .....	1
1.1 Bathymetric Needs for Shipping .....	3
1.2 Bathymetric Needs for Wave Energy Convertors .....	6
Chapter 2: Literature Review .....	8
2.1 Origins of Topography .....	9
2.2 The Progression of Underwater Mapping .....	11
2.3 Basic Principles of Sonar and LIDAR .....	13
2.3.1 SONAR .....	14
2.3.2 LIDAR .....	20
Chapter 3: Objectives and Assumptions .....	25
3.1 Challenges .....	25
3.2 Assumptions .....	28
Chapter 4: Case Study .....	30
4.1 Site Selection .....	31
4.2 Data Acquisition .....	33
4.2.1 USGS Bathymetry Data .....	34
4.2.2 USGS Side-Scan SONAR Bathymetry Data .....	36
4.2.3 ABL Data .....	37
4.3 Position Accuracy .....	39
4.4 Qualitative Analysis .....	41
4.5 Data Merge Analysis .....	50
4.6 Quantitative Analysis .....	54
Chapter 5: Conclusions .....	69

5.1 Discussion .....	71
5.2 Future Work .....	74
References.....	77
Biography.....	82

## LIST OF TABLES

Table	Page
Table 1 Variables and Impact to SONAR/LIDAR Bathymetric Collecting .....	27
Table 2 Interpretation of Moran's I Output (ESRI, 2015) .....	56

## LIST OF FIGURES

Figure	Page
<b>Figure 1 Changes in beach profiles between summer and winter caused by changes in wave climate. During winter storms, the beach is eroded and seaward cross-shore sediment transport results in the formation of offshore bars (Purkis, 2011) .....</b>	2
<b>Figure 2 Average and Maximum Vessel Size 2009-Present (Source: BlueWater Reporting) .....</b>	5
<b>Figure 3 Number of Container Ships Worldwide by Ship Size (mid-2010) .....</b>	6
<b>Figure 4 Initial Ping from Towed SONAR “Fish” .....</b>	15
<b>Figure 5 Return Sonar Ping from Towed SONAR “Fish”; light cone is ½ of swath area .....</b>	15
<b>Figure 6 Return from SONAR Pings .....</b>	16
<b>Figure 7 Return from SONAR Pings for Collection and Processing .....</b>	16
<b>Figure 8 Return from SONAR Pings for Collection and Processing .....</b>	17
<b>Figure 9 Benthic Tools over Time (NOAA, NOAA Office of Coast Survey, 2014) ..</b>	19
<b>Figure 10 Scattering Coefficient, Absorption and Total Attenuation of EM radiation (wavelengths) in Pure Water (data from (Bukata, 1995)) .....</b>	21
<b>Figure 11 Basic Airborne LIDAR (Kvietk, 1999) .....</b>	23
<b>Figure 12 Proper method of taking a Secchi disk reading (Davies-Colley, 1993)....</b>	27
<b>Figure 13 Block Flow Diagram Outlining Thesis Analysis Process. Numbers in parenthesis indicate section numbers in this chapter. ....</b>	30
<b>Figure 14 Rhode Island Area of Interest (data developed from ArcMap) .....</b>	33
<b>Figure 15 Sonar Data Visualization; Rhode Island .....</b>	42
<b>Figure 16 Side-Scan Sonar Data Visualization; Rhode Island .....</b>	43
<b>Figure 17 ABL Data Visualization; Rhode Island .....</b>	44
<b>Figure 18 Sonar data visualization, Rhode Island case study area; In this figure depth values are visualized by color, from low depth (dark red) to high depth (dark blue) .....</b>	46
<b>Figure 19 Side-Scan Sonar Data Zoom Visualization; Rhode Island; In this figure depth values are visualized by grey level values, from low depth (white) to high depth (black) .....</b>	47
<b>Figure 20 ABL Data Zoom Visualization; Rhode Island; Legend values are in meters and there are two color scale bars as there are two data sets side by side in this figure .....</b>	48
<b>Figure 21 SONAR, Side-Scan SONAR and ABL Data Zoom; Rhode Island .....</b>	49
<b>Figure 22 Sonar Data with Wrecks Zoom to Ship (1:3889); Rhode Island .....</b>	50



<b>Figure 23 Image Generated from Mosaic of Side-Scan Sonar and ABL; Rhode Island; In this figure depth values are visualized by grey level values, from low depth (White) to high depth (Black).</b>	<b>53</b>
<b>Figure 24 Z-scores and P-values associated with the standard normal distribution (ESRI, 2015).</b>	<b>55</b>
<b>Figure 25 Moran’s I Calculations (ESRI, 2015).</b>	<b>57</b>
<b>Figure 26 Moran’s I Executed on SONAR (ArcGIS 10.2.2)</b>	<b>58</b>
<b>Figure 27 Moran’s I Executed on Side-Scan SONAR (ArcGIS 10.2.2)</b>	<b>59</b>
<b>Figure 28 Moran’s I Executed on ABL (ArcGIS 10.2.2)</b>	<b>60</b>
<b>Figure 29 Getis-Ord General G Calculations (ESRI, 2015).</b>	<b>62</b>
<b>Figure 30 Getis-Ord Gi* Calculations (ESRI, 2015)</b>	<b>63</b>
<b>Figure 31 SONAR Hot Spot Analysis with Rendering (ArcGIS 10.2.2)</b>	<b>64</b>
<b>Figure 32 Example Inputs and Output from Zonal Statistics (ESRI, 2015)</b>	<b>65</b>
<b>Figure 33 Example Inputs and Output from Zonal Statistics; Legend measurements are in meters</b>	<b>66</b>
<b>Figure 34 Moran’s I Executed on Range Zonal Analysis (ArcGIS 10.2.2).</b>	<b>68</b>
<b>Figure 35 An Oyster Wave Energy Converter Device (Flatley, 2009)</b>	<b>74</b>

## **ABSTRACT**

### **A COMPARATIVE ANALYSIS OF SHALLOW WATER MAPPING TOOLS**

Geoffrey S. Cleveland, M.S.

George Mason University, 2015

Thesis Director: Dr. Arie Croitoru

Varied needs have encouraged development of different technologies over time to meet those needs inclusive of technologies to map land, oceans and shorelines. Over the last decade significant effort has been put into fusing the area that joins the land maps to ocean benthic (ecological region at the lowest level of a body of water such as an ocean or a lake) maps so there is a continuous topographic view. There are several methods used to define the topography of underwater regions such as ship based single and multi-beam echo-sounder approaches with the latter providing complete high resolution coverage of the sea floor. (Committee on National Needs for Coastal Mapping and Charting, 2004). The goal of this thesis is to assess a group of common tools for mapping underwater topography, also known as bathymetry, for use in fusing the land topography to the sea floor topography. Data will be collected from web resources and unclassified geospatial databases for this research and key technical areas and weaknesses will be assessed to draw conclusions. The result of this analytic research

identifies a recommended tool for shallow water bathymetry collection and provides recommended applications to support wave renewable energies.

## CHAPTER 1: INTRODUCTION

Today's LIDAR technology allows us to capture land topography, while oceanic shorelines and some underwater topography are being captured through different types of SONAR or other approaches. A key gap at this point in bathymetric mapping is the area *between* the deep sea mapped area and the areas of the landmasses that are mapped – the shallow water areas between rivers and shorelines as well as beaches and oceans are also included for overall continuity. As we are currently dealing with the challenges to be able to fuse the data sets between topographic mapping above sea level and bathymetric mapping below sea level it is a developing science and, over the last decade, has improved steadily.

Knowledge of coastal elevation and shallow shoreline and riverbed topology is an essential requirement for resource management, scientific research and, of course, for military applications. This information is also essential for ship to shore movement, tracking changes in shorelines that may require defense from flooding and erosion, and identifying regions that may require environmental protection – they all rely on accurate and repeated characterization of benthic communities and morphology (Brock, 2009). However, large areas of the world's coastal marine environments remain poorly characterized because they have not been mapped with sufficient accuracy and at spatial resolutions high enough to support a wide range of societal needs (Costa, 2009). The

fundamental information that would be provided with shallow water data could support a better understanding of near shore geomorphology (Finkl, 2005), assessment of impacts from storms and tsunamis (Matsuyama, 1999), support for the development of hydrodynamic models (Irish, 1998), information to enable transport and associated dredging (Wang, 2007), information to enable management of fishing wildlife (Nishida, 2001) to identify a few uses that are significantly improved with the shallow water bathymetry. For military applications, there is a need to map and understand obstacles for ship-to-shore operations, so there are clear ingress and egress paths of attack and escape for ship to shore vehicle movements. In both civilian and military areas, shallow water mapping has emerged as a significant need and, as can be seen in the Figure 1 below, which identifies variances in ocean shorelines merely from the impact of changing seasons which can directly cause boating safety concerns.

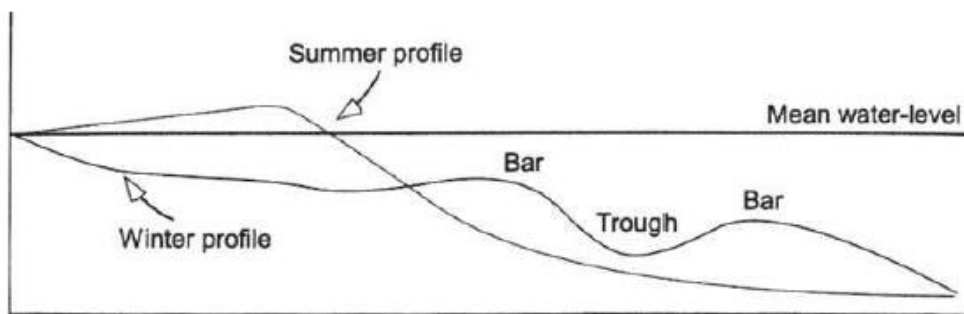


**Figure 1 Changes in beach profiles between summer and winter caused by changes in wave climate. During winter storms, the beach is eroded and seaward cross-shore sediment transport results in the formation of offshore bars (Purkis, 2011)**

This shallow water mapping need also drives a growing desire for tools and analysis approaches which provide data to document and explore the full range of spatial and temporal variations in shoreline and river systems which discriminate between land and water using all available channels in SHOALS, Light Detection and ranging (LIDAR) techniques, combined with Global Positioning System (GPS), and any additional combinations from SONAR or other data that make it possible to obtain accurate, continuous topological to bathymetric maps. These images, and possible separate combinations of data collected from different tools, can then be assessed and analyzed for the multitude of purposes each user specifically desires.

A continuous land to deep sea mapping knowledge requirement is becoming more of a shallow water mapping science, which has grown at a rapid rate in recent years to include a multitude of analysis tools and approaches. There are several shallow water mapping tools and techniques currently used to perform shoreline and shallow water depth mapping. Motivated by these developments, the objective of this research is to review SONAR and LIDAR tools, assess how the tools work and review their limitations such as use in salt water, fresh water, turbulence, etc. With analysis of the above, the results will provide a recommendation on what tool would be preferred to utilize for shallow water mapping and/or which “tools” based on the environment they are used in.

### **1.1 Bathymetric Needs for Shipping**

According to the American Association of Port Authorities (AAPA) (<http://www.aapa-ports.org/Industry/content.cfm?ItemNumber=1032>) there are some 360

commercial ports that provide approximately 3,200 cargo and passenger handling facilities.

Currently, there more than 150 deep draft seaports are under the jurisdiction of 126 public seaport agencies located along the Atlantic, Pacific, Gulf and Great Lakes coasts, as well as in Alaska, Hawaii, Puerto Rico, Guam, and the U.S. Virgin Islands. During the first five months of 2012, the 63 U.S. ports (out of 82 surveyed) that returned completed AAPA Port Infrastructure Investment questionnaires reported that they, and their private-sector business partners, planned to invest an estimated \$46 billion for infrastructure during the five-year period between 2012 and 2016. A large part of infrastructure funding includes monies to attain safety of navigation, dredge planning, dredging and other analysis requirements through the use of bathymetry to keep and maintain operation of this \$4.6 trillion industry - noting that this figure represents 26% of the nation's \$17.4 trillion economy in 2014 (Martin, 2014).

Many East Coast ports have started dredging to increase harbor depths to accommodate larger vessels. For reference, the largest containerships on both the Asia-North Europe and transpacific trades in early 2009 belonged to Maersk Line, with respective capacities of 14,781 twenty-foot Equivalent Units (TEUs) and 9,700 TEUs; TEUs being a the volume of a 20-foot-long (6.1 m) inter-modular container – the number of TEUs being the amount of these large metal containers that can be loaded. Since 2009, average vessel size between Asia and North Europe has increased 65 percent to 11,769 TEUs, and the largest containership currently in service, the MSC Oscar, can hold 19,224 TEUs, an increase of 30 percent from 2009 (Meyer, 2015). The larger vessels sizes over

time which the Figure 2 identifies require deeper drafts to float, driving up the need to understand and manage the bathymetric areas that these huge shipping vessels are traversing over.

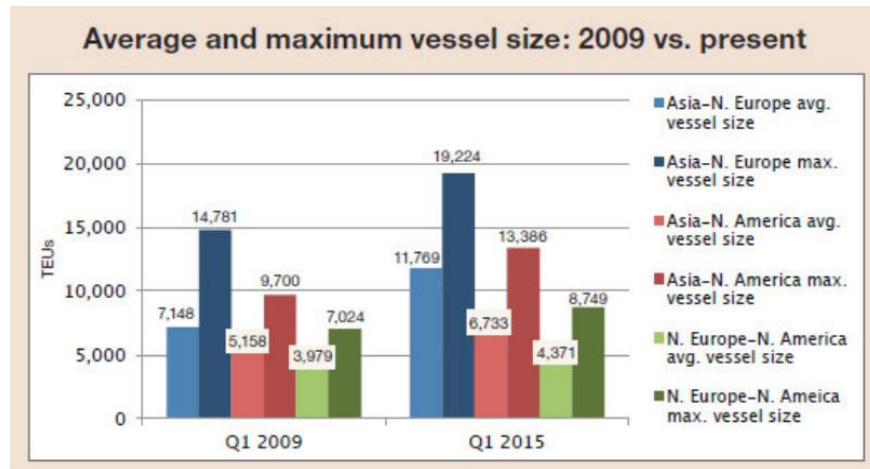


**Figure 2 Average and Maximum Vessel Size 2009-Present (Source: BlueWater Reporting)**

To provide an idea of the amount of movement that is going on within the shipping industry, Figure 3 provide statistics from Statista.com which outlines the magnitude of numbers and sizes of these colossal vessels that are supported through the use of bathymetric analysis tools.



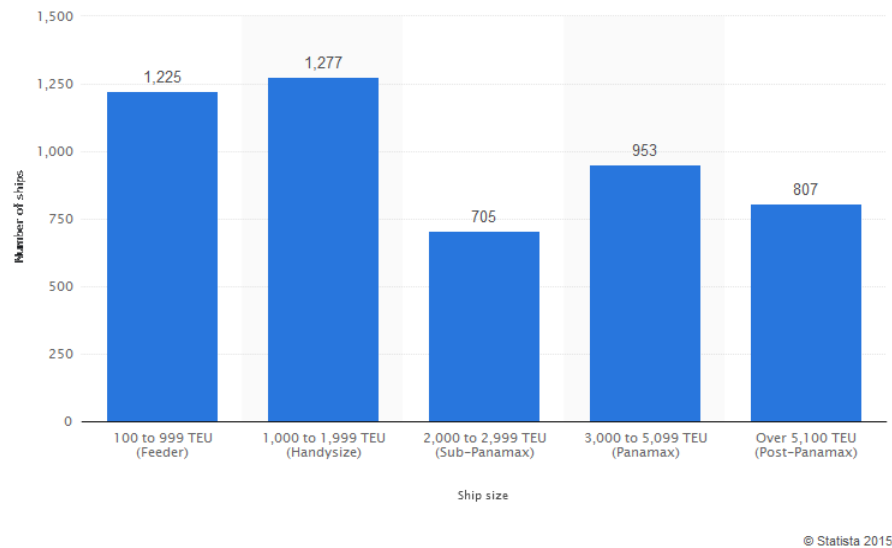


**Figure 3 Number of Container Ships Worldwide by Ship Size (mid-2010)**

## 1.2 Bathymetric Needs for Wave Energy Convertors

Although shipping is one of the areas requiring bathymetry, Wave Energy Conversion (WEC) techniques do as well. WEC technology is a green energy arena that is a growing field among the many that look to harness energy from the sea. There are a multitude of WEC technologies which are a near shore technological approach for WEC that has many competitors such as far shore, floating and submerged technologies. The total global offshore wave energy potential has been evaluated to be up to 10TW, which is sufficient for world energy demand (Panicker, 1976) which, in itself, is a foundational metric attracting investment in this technology. Each of these WEC technologies has their specific requirements for implementation that a good reference understanding of underwater topography would support (Simon P. Neill, 2013) (Clement, 2002).

Bathymetry can support identification of WEC placement and explaining the nature of

the near-shore waves (Ram, 2014) which correlate the amount of energy that the WEC can provide so not only would a benthic area that is flat potentially be ideal to identify if it is a WEC gravity moored device, one with bedrock may be necessary for mounting the device or a location that has a specific elevation to optimize the wave technology being implemented based on tidal activity for higher energy output.

In short, the bathymetry is necessary for both navigation and design of WEC applications. The fundamental need to know bathymetry for ships traversing waters transporting cargo and where and what foundation would provide optimal placement of WEC technologies in the optimal associated wave area is where the desire to better understand bathymetric tools originated and initiated the scientific research for this Thesis.

## **CHAPTER 2: LITERATURE REVIEW**

The history of human progression and development has presented opportunities to advance how people move and navigate around the world. It started on foot and then progressed to riding animals and sailing ships, leading to current methods of moving people and goods quickly by driving vehicles, flying planes, taking trains and even still, riding bicycles. While these advances have made significant changes in our capacity to traverse the globe, the ability to effectively and safely use waterways has retained its historic role as a key method of transportation over large distances. Consequently, the demand for reliable information about waterways, and in particular bathymetric mapping is still strong today in order to understand what vessels, with associated drafts (depth of water to float a ship), can safely traverse which waters. As discussed in the introduction the U.S. shipping is growing in size, between 1970 and 2010, developing countries share in the volume of seaborne imports rose from just 18 per cent to 56 per cent of the world's total (Kunatch, 2011) - all of these vessels travelling to hundreds of sea ports across the world (CIA, 2015) requiring the same bathymetric needs. Addressing this need, recent developments in Light Detection and Ranging (LIDAR) and SOund Navigation and Ranging (SONAR) have opened new opportunities for more accurate and timely bathymetric mapping. Through the use of LIDAR, surfaces (e.g. terrain) can be captured with better resolution and detail, offering a cost-effective

alternative to the more traditional methods surveyors of years past could ever hope to attain.

Both the land and the deep water topographic data collections have not been effectively fused together. As a result, there is an ongoing challenge of being able to provide shallow water bathymetry for a continuous land view, above and below water. This need has brought about new techniques and methods including airborne laser use and other multi-beam laser approaches. Motivated by this development, this research analyzes the currently available bathymetric methods of Sonar and LIDAR touching on variances such as ship-based multi-beam SOUNd Navigation And Ranging (SONAR), single beam SONAR, Airborne Laser (ABL) light detection and ranging Bathymetry, and vertical beam echosounder (VBES) bathymetric approaches to assess their advantages and limitations for shallow water bathymetry. The hypothesis is that the ABL technology is the preferred mapping approach for capturing topographic features in bathymetry.

## **2.1 Origins of Topography**

The mapping of the environment has long been practiced by mankind – although it may have been in a very primitive form of cave painting using pigment from leaves and flowers mixed with water for color variations or possibly in the form of a fine mural tile generated by a Roman artisan to depict a city, streets and associated features of an area – it was a planned execution by those people to both provide a visual representation with some orientation for guiding people in and around areas with reference points as well as enlightening them to their surroundings based on fundamental, often eye catching, cartography. In ancient history there may not have been a need to map large areas as the

human inhabitants in those times did not have domestic animals to ride and rarely ever travelled outside of a radius of five or ten miles. As time progressed and animals started being used for travel the need to have some type of map or representation of larger geographical spaces emerged. Maps were primarily used for understanding the lands being traveled, and were associated with some landmarks to navigate by – likely the first true need that drove some cartography in a regulated fashion for common use.

Throughout history shipping was a primary way of shipping goods along coastlines and across oceans, as it was much easier to transport large quantities of goods over water than over land. With this need, water navigation came into the fold needing to understand the what and the how of the continents and shorelines. Water navigation began to have some importance for understanding which cities and continents are within those shorelines and what associated major waterways for travel and trade could be used to get to those locations, in order to meet the navigational needs for supporting shipping commerce in North America. A survey of the coast was initiated and became known as the U.S. Coast Survey charting over 3.4 million square nautical miles of water and 95,000 miles of shoreline, as well as alerting mariners to the depths and dangers along the 200 mile zone adjacent to the U. S. coastline, an area known as the Exclusive Economic Zone (NOAA, 2013) .

The history of the origins and methodologies imposed for mapping can be tracked from several sources. Perhaps it was René Descartes' (1596–1650) with his works *Discourse on the Method* or Pierre de Fermat (1601–1665) with his research on curves and their geometric solutions; the resulting path was a brilliant tie from fundamental

geometry to coordinate system mapping (Newman, 1956) – the origin from which, arguably, genuine cartography in two and three dimensions grew to being a highly reliable and accurate methodology of identifying reference points in a coordination system and visualizing them through a map.

The ability to take these mathematical approaches and to bring them into more defined structure with additional variations for visualization in both the 2D and 3D environments has eventually converged over the last few hundred years to a highly reliable methodology of identifying reference points in a coordinate system and providing visualization not only as historically was available on a parchment of paper in two dimensions but a full three dimensional view to yield an almost real display of the sampled topographic environment – even where you are be able to sit at a computer and zoom in and out of a 3D map, something unheard of just 20 years ago.

## **2.2 The Progression of Underwater Mapping**

Until the latter half of the 20th century, Lead lines, ropes or lines with depth markings and lead weights attached were lowered from ships into the water and read manually in a labor-intensive and time-consuming process to estimate depths (Calder, 2006). The depths were compiled on charts to give a coarse-scale representation of the seafloor and identify navigation hazards. Advances in technology led to the use of single beam and multi beam SONAR and echo-sounding allowing better bathymetric mapping. More recently, elevation point clouds attained from LIDAR surveys provide detailed coverage of the land topography and, using various frequencies, are currently in use to assess benthic regions as well.

In the early years of World War I (WWI) the British civilian and military shipping routes were being repeatedly attacked and destroyed by German submarines – the famous U-Boats. A recent development that allowed for the British to track aircraft through wave propagation in the air called RADAR lead to the theory and experimentation of wave propagation in the water. The ability for the British to start tracking submarines started with the use of hydrophones in 1917 which allowed some detection of the submarines but did not provide distinct enough information to be able to detect, close and engage with them. Moving forward with the technology, ultrasonic echo detection was developed. This echo detection approach gave not only distance but bearing of the vessels so the submarines could be engaged by the British (Jones, 1985). The British referred to this ultrasonic approach as the Anti-Submarine Detection Investigation Committee (ASDIC) which was the beginnings of what was developed from around the 1930s until now as what we understand to be SONAR.

This wartime technology – although not intended to be a geospatial tool initially, has developed into both a military and non-military geospatial tool. For Military applications it allows for submarines to understand the terrain and objects around them or ships to visualize what is underneath the water levels they are cruising through, enabling these vessels to map out and have confidence in the shipping routes and their associated depths. In the Non-military applications SONAR has provided several non-military uses which include fish finding, depth sounding, and, most importantly for the purposes of this Thesis, mapping of the ocean floor.

The U.S. Army Corps of Engineers (USACE) developed the Scanning Hydrographic Operation Airborne LIDAR Survey (SHOALS) system, which utilizes a multi-beam laser surveying approach using both green and infrared wavelength pulses to determine the water surface level and the ocean floor topography (Wozencraft, 2003). Since the USACE field test of SHOALS in 1994 to collect water depths in navigation channels for dredge payment, the SHOALS concept has been improved with changes in frequencies used and software adjustments to improve data collection processing (Wozencraft, 2003).

Bathymetry mapping has been undergoing a revolution driven by the invention and evolution of new imaging and navigation technologies for over a quarter century now. Side-Scan sonar, multibeam bathymetry, satellite altimetry and Global Positioning System (GPS) are at the forefront of an array of tools that enable the seafloor to be ‘seen’ to a greater level of detail than ever before. These recent advances in seafloor bathymetry can now rival or surpass those available for the terrestrial environment (Iampietro, Kvitec, & Erica, 2005).

### **2.3 Basic Principles of Sonar and LIDAR**

In order to perform proper analysis, the fundamental understanding of how Sonar and LIDAR are utilized will be discussed in this section. The purpose of this chapter is to review the principles of SONAR and LIDAR and introduce this fundamental knowledge to the reader for conceptualization with enough depth that the follow on case study and analysis of these tools will be clear.



### **2.3.1 SONAR**

Sonar developed from underwater acoustic research during World War I and was the first sustained scientific and technological response to a new weapon system, the submarine (Hackmann, 1986). The primary use for SONAR was for detecting and locating objects especially underwater by means of sound waves sent out to be reflected by objects. Essentially a sound wave is emitted from a source, impacts an object and is reflected back, received and the collected wavelengths were assessed to identify objects.

The Side-Scan Sonar was developed by the Institute of Oceanographic Sciences (IOS) in the United Kingdom, with the additional capability of mapping the texture of the seabed, and cutting wider swaths than the single beam sonar. Although Side-Scan Sonar is currently used to accurately image large areas of the ocean with the acoustic beam being very wide in the sideways direction and very narrow in the forward direction, it is a specialized system for detecting objects on the seafloor. Most side scan systems cannot provide depth information. Figures 4-8 are images that were created to visualize and outline the process showing a submerged Sonar “fish” in tow behind a boat generating Side-Scan Sonar and Vertical Beam Sonar pulses also referred to as “pings”.

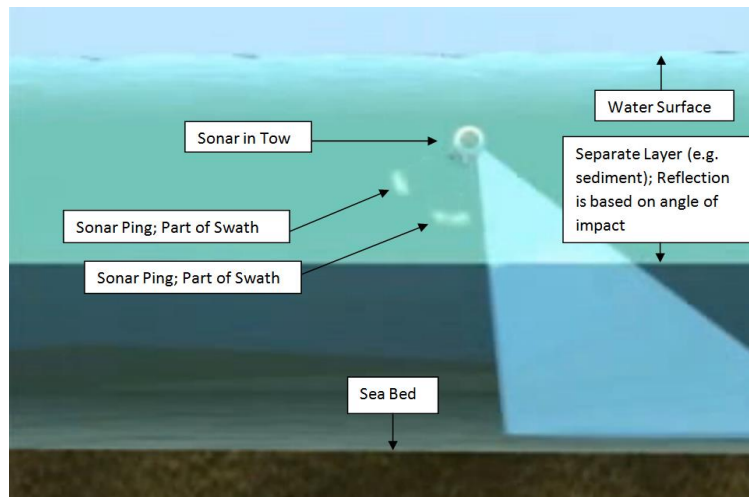


**Figure 4 Initial Ping from Towed SONAR "Fish"**

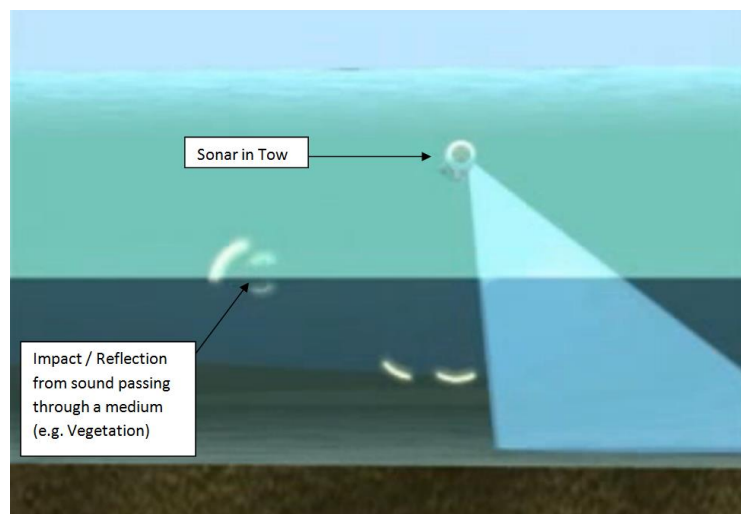


**Figure 5 Return Sonar Ping from Towed SONAR "Fish"; light cone is  $\frac{1}{2}$  of swath" area**

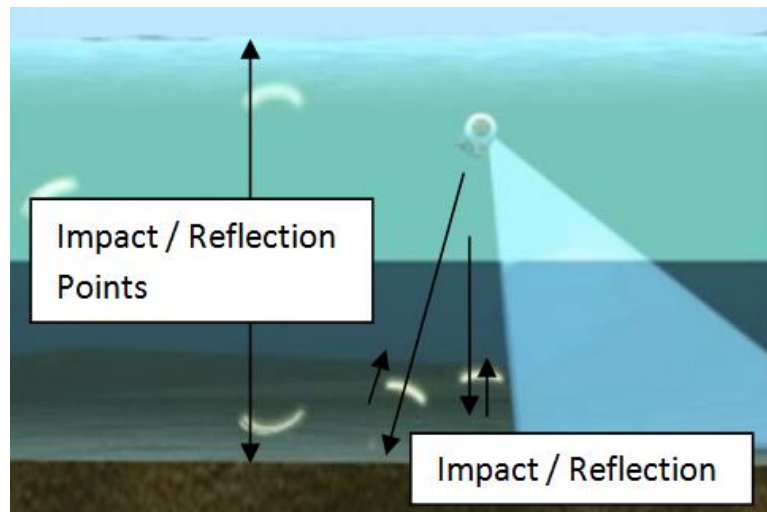


**Figure 6 Return from SONAR Pings**

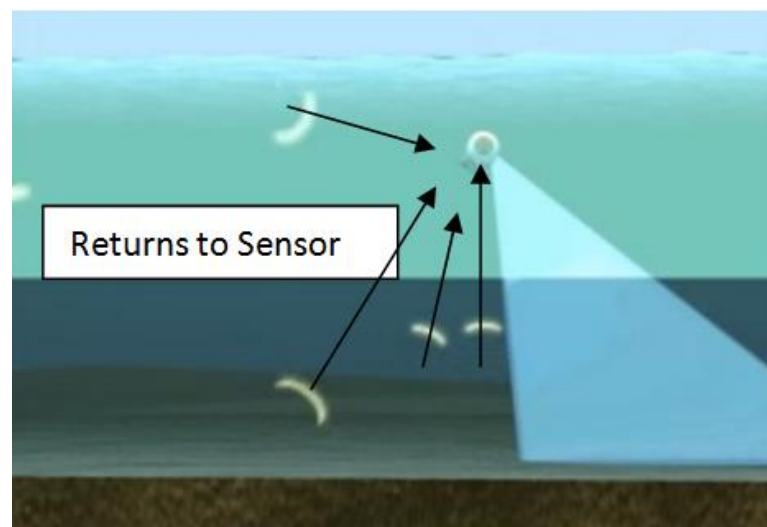


**Figure 7 Return from SONAR Pings for Collection and Processing**

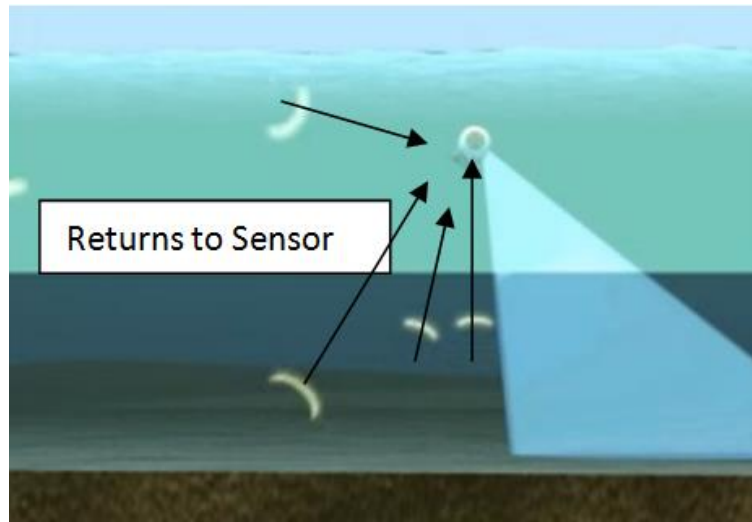


**Figure 8 Return from SONAR Pings for Collection and Processing**

In visualizing the images it is clear that a "swath-sounding" sonar system is used to capture information in a line extending outwards from the sonar transducer. Systems acquire data in a swath at right angles to the direction of motion of the transducer head. As the head moves forward, these profiles sweep out and collect data on a ribbon-shaped surface of depth measurement, perpendicular to the movement of the transducer "fish" direction, known as a swath. Each "ping" from the sonar provides a swath or ribbon of data. By pinging continuously, driving the boat in straight lines, and laying all the ping raw data records next to each other it provides an image which essentially yields a vertical profile through the water column and benthic area.

Single beam echo sounders collect bathymetric soundings in a swath by electronically forming a transmit and receive beam in the transducer hardware which measure the depth to the sea floor. Multibeam echo sounders (MBES) collect bathymetric soundings in a swath by electronically forming a series of transmit and

receive beams in the transducer hardware which measure the depth to the sea floor in discrete angular increments or sectors across the swath (Hughes-Clarke, 1996). Both Single Beam and Multi Beam SONAR methods are generally mounted to the hull of a vessel and data is collected perpendicular to the direction of travel. Various transmit frequencies are utilized by different MBES systems depending on the sea floor depth. The simple seabed multi-beam configuration may consist of two echo sounder transceivers, one with low frequency and one with higher frequency, for example, low frequency (12 kHz) systems can collect swath soundings at full ocean depths, many up to 10,000 meters; In contrast, high frequency MBES systems (300+ kHz) are utilized for collecting swath bathymetry in depths of 20 meters or less (USGS, 2014). MBES systems which utilize multiple transducers provide a more detailed view of the ocean floor than a single beam sonar system.

Surveys with single beam sonar systems represent an effective method of covering and mapping areas in a relatively short time with greater detail than the historically used Lead line method and as time progressed, the advent of multi-beam sonar allowed us to cover increasingly wide areas in a relatively short time with increasing accuracy of the benthic areas in review. Figure 9 provides a visualization of these tools and the variance of area that can be covered with advances in technology over the last century.

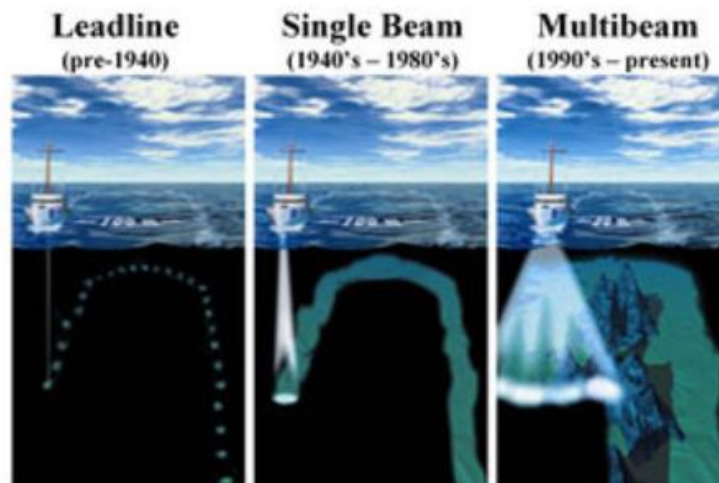


**Figure 9 Benthic Tools over Time (NOAA, NOAA Office of Coast Survey, 2014)**

Multi-beam bathymetric mapping systems are straightforward in that they consist of a source transducer designed to ensonify a broad region out to either side (e.g. 60 degrees out to either side, but only one or two degrees along the ship's track). They also involve a receiver array (hydrophones) that, through the magic of phase delay techniques, manages to form multiple adjacent beams focused at known angles. As each 'beam' listens for returns from only one angle, but every beam records the time of the returning echoes independently, each “ping” results in "n" pairs of range ( $((\text{travel time} \times \text{speed of sound}) / 2)$ ) and angle, where n is the number of beams. There is a difference between the speed of sound in air and water, with the speed of sound in water being about 4.3 times as fast than in air (Bilaniuk & Wong, 1993), however, this is a variable addressed within the collection algorithms. Range and angle for each beam can be converted to cross-track distance and depth. Combining all the points together results in a bathymetric surface.

It is important to note the collection of returns and mapping of those points from sonar pings is not so fundamentally easy as send a signal, get a signal and map the points together to define a surface area. Generally, any sonar data collection includes seafloor backscatter, which is the amount of acoustic energy being received by the sonar after a complex interaction with the seafloor – these are not direct collections, but as noted “scattered” returns that have been becoming recognized more and more as an invaluable tool. The backscatter data can be used to determine bottom type, because different bottom types “scatter” sound energy differently. For example, a softer bottom such as mud will return a weaker signal than a harder bottom, like rock. The backscatter, as is noted, can provide additional data and insight into the environment especially if the data points are georeferenced together with the timed sonar collections for bottom location.

### **2.3.2 LIDAR**

The term LIDAR (Light Detection And Ranging) was coined by James Ring (Ring, 1963), as a remote sensing technology that measures elevation or depth by analyzing the reflection of pulses of laser light off an object.

LIDAR technology is based on pulses of laser light (light constrained to a particular wavelength) that are aimed at an object, and the time it takes for the reflected light beam to return to a sensor it is measured. The time is then converted into distance. Because laser pulses travel at the speed of light, any slight difference in two successive pulse returns is almost imperceptible, yet measurable and allows technology to make calculations and measure distances.

In recent years, Airborne Laser Scanning (ALS) systems have been applied to a wide array of terrestrial applications such as mapping out bare earth topography or utilizing it for archaeological applications (Crutchley, 2010). Generally, the ALS spectrum operates in the near or short wave infrared wavelengths (in the range of 1064-1550 nm) which have been found to be largely absorbed by water bodies (Curcio, 1951). Due to the absorption at these wavelengths the utility of conventional ALS systems for bathymetric use is greatly limited. Through testing, alternative wavelengths were found to be more suitable for mapping benthic areas as identified in Figure 10 outlining electromagnetic (EM) radiation propagates in clear water based on absorption and scattering coefficients.

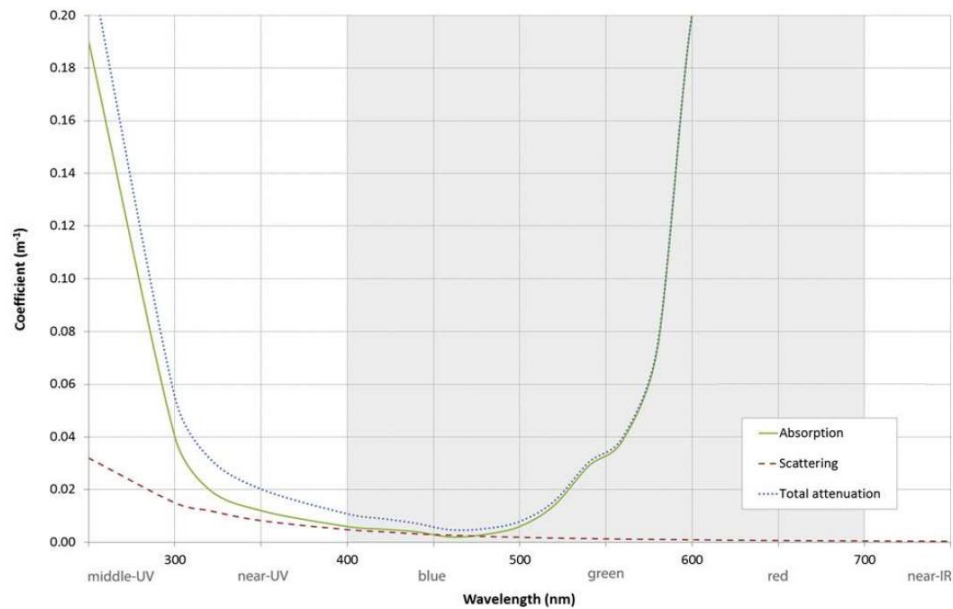


**Figure 10 Scattering Coefficient, Absorption and Total Attenuation of EM radiation (wavelengths) in Pure Water (data from (Bukata, 1995))**



Through understanding the absorption and reflection of the EM radiation in water a method was developed and is currently a foundational approach for benthic LIDAR Systems to use laser pulses generated and received at two frequencies. A higher frequency infrared (IR) pulse is reflected off the sea surface (generally in the “red” wavelength); while a longer wavelength green laser penetrates through the water column and reflects off the bottom as can be referenced in Figure 11. Analyses of these two distinct pulses are used to establish water depths and shoreline elevations. With good water clarity, these systems can reach depths of 50 meters (NOAA Office of Coast Survey, 2014) and can produce 10 to 15 centimeter vertical accuracy at a spatial resolution greater than one elevation measurement per square meter meeting the requirements of many coastal research and management applications (Klemas, 2011). There are multiple methods to implement LIDAR with the most common method for purposes of bathymetry being aviation mounted platforms and will be the type discussed in this Thesis.

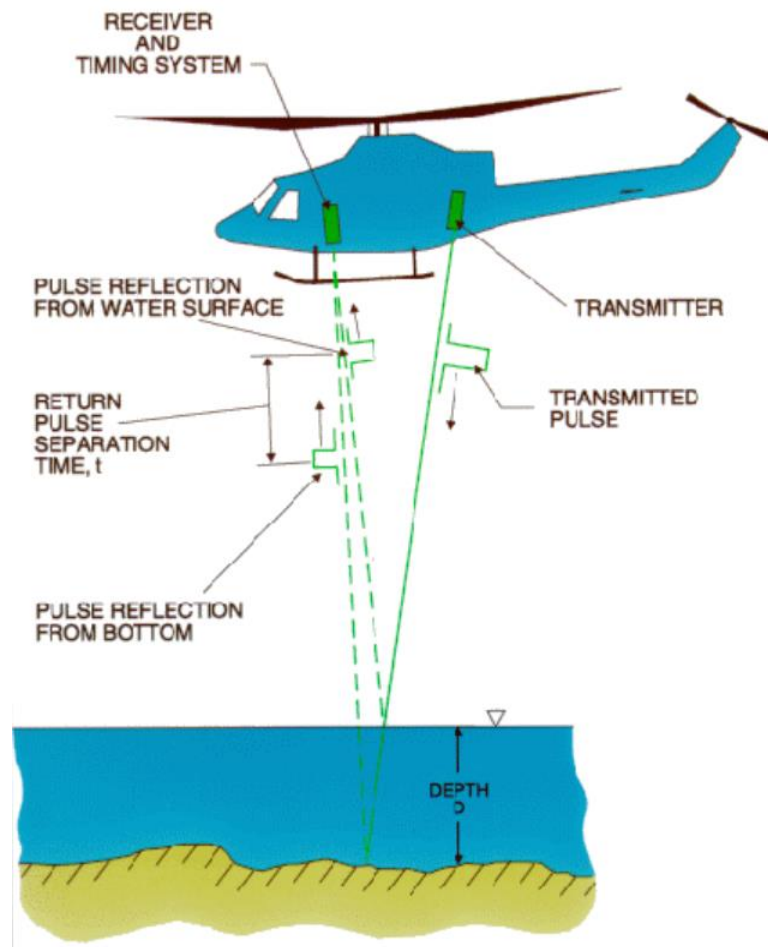


**Figure 11 Basic Airborne LIDAR (Kvietk, 1999)**

Airborne Bathymetric LIDAR (ABL) may not have been initiated as a safer approach to bathymetric mapping but it is used to acquire data in areas with complex and rugged shorelines where surface vessels cannot operate efficiently or safely because of rocks, kelp or breaking surf. Some examples of these areas include Alaska, the North Atlantic Coast and the Caribbean. Additionally, ABL platforms are much faster and cheaper to implement to attain mapping data so they are increasingly becoming a tool to

fill the mapping gap between topographic and bathymetric zones that have historically been mapped through sonar approaches.

As LIDAR accuracy is susceptible to water turbidity it is preferred to execute boat reconnaissance to monitor water clarity prior to commencement of airborne survey operations. The reconnaissance is to use Secchi disks to determine water clarity and identify when water clarity is deemed adequate for aerial LIDAR collection.

## CHAPTER 3: OBJECTIVES AND ASSUMPTIONS

The objective of this Thesis is to perform a case study between Airborne Bathymetric Lidar (ABL), Side-Scan SONAR and SONAR. Qualitative and quantitative assessments are made between the data sets and a data set merge is developed to validate the concept of joining multiple data sets. Qualitative analysis will visually be analyzed as most users of commercially available data will utilize the data collected in this fashion without modification. A merge between Side-Scan SONAR and ABL data is then provided validating the merging of multiple data sets to output a continuous surface from land through to bathymetric regions. Qualitative analysis is provided for the data sets and statistical analysis and assessments is reviewed with detail.

### 3.1 Challenges

There are a multitude of approaches to obtaining data for terrestrial, deep water and shallow water terrain mapping. The ones that are to be explored in this research includes different approaches of using *laser* (at different wavelengths) and *acoustic* methods. With the use of wavelength propagation through shallow water there are some limitations that can impact the data quality, which can potentially result in incomplete data or areas where data is not collected at all, (also called “holes”). Several bathymetry-specific factors contribute to the ability and probability of detecting underwater mapping terrain. Bathymetric laser returns can be impacted by water depth, turbidity (cloudiness

caused by suspended or dissolved material), salinity, wave activity, and algae blooms, as each of these factors can affect water clarity - which is required, under optimal conditions, to enable the signal and returns to yield accurate data (Coleman, 2011). Most of the variables that can impact laser returns can be avoided by selecting collection timeframes that mitigate data impact variables such as when there will be little or no water turbidity, or when the Secchi depths, a measure of the cloudiness or turbidity of surface water, are very high.

To provide a better understanding of the Secchi tool, the original Secchi disk, as created in 1865 by Angelo Secchi, is a plain white circular disk roughly 12 inches in diameter. Currently there are a multitude of variations of this disk but the most common is an 8 inch diameter metal plate painted with an alternating white and black color pattern used to measure water transparency in bodies of water. The disc is mounted on a pole or line, and lowered slowly down in the water to the depth at which it disappears from view. The depth at which the disk can no longer be seen is the Secchi depth that is recorded and provides a tool to assess how much potential interference (turbidity, salinity, algae, etc.) impacts the effectivity of SONAR and LIDAR tool data collection. The method of utilizing a Secchi disk is provided in Figure 12.

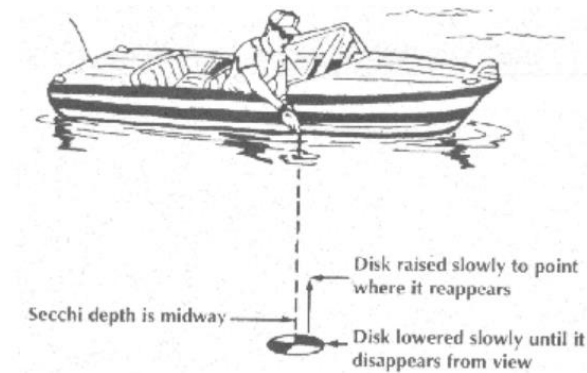


**Figure 12 Proper method of taking a Secchi disk reading (Davies-Colley, 1993)**

A detailed chart of high impact variables and associated mitigation approaches is provided in Table 1, time and research progress will provide additions to this table and modify it based progress of Remote Sensing Tools, and their limitations that come into play. Understanding variables and their impact allow pre-planning, thus enabling better probability for high accuracy collections which can be utilized for analysis and integration into and between ground mapped data as well as underwater SONAR mapped areas.

**Table 1 Variables and Impact to SONAR/LIDAR Bathymetric Collecting**

VARIABLE	IMPACT	MITIGATION
Saltwater	Variable	Sample during non-turbid environment; Secchi testing

Algae	High	Sample during cold season when Algae is not in full effect
Water Depth	Constant for specific wavelengths	Utilize different wavelengths to support depths; understand depths being sampled
Water Debris	Variable	Sample during non-turbid environment; Secchi testing
Gas	High Impact to Sonar	CO2 leakage monitoring on the seabed – is this a risk to collection??
Collection Location Risk (e.g. rugged shoreline)	High Impact to Sonar	Assess with alternate collection tools (e.g. LIDAR)

### 3.2 Assumptions

Assumptions going into the review of Bathymetric tools and associated components are critical to restrain the variables that must be limited in order to focus the analysis. The intent is to create constraints such that the remaining variables provide the ability for assessing the core topics of this Thesis.

The following assumptions will be utilized throughout cast study:

- Data collected is assumed to have been collected under optimal conditions.
- For this research it will be assumed cost is not a factor when procuring the components for data collection.

- The memory requirements (noting again, that multi-beam data has much more data density and requires more storage than single-beam data), processor requirements, and video requirements are also not factors and assumed to be met by whatever cost model is being used as these components are assumed not to impact the core data collection capabilities.
- Size, weight, and power are generally core systems engineering concerns whenever integrating any device into a platform for use. Both airborne and shipboard integration can generally provide ample support in these arenas so they will be assumed components of the cost model as well.
- The assumption the connectivity between the components and the data collection hardware is part of the cost model integration so there will be no detail on what connectivity is required (e.g. RS-232, Ethernet).
- The final assumption is that the multi-beam LIDAR will be the preferred bathymetric approach noting all other assumptions made.

Future Cost as An Independent Variable (CAIV) analysis is recommended to provide cost component input with life-cycle cost–performance–requirements tradeoffs for individual applications.



## CHAPTER 4: CASE STUDY

Without the capacity to collect data independently, data was gathered and assessed for overlap in order to enable the comparative analysis. In particular, regions of overlapping data were used for site determination to enable analysis within a common area of interest that contains the same features for assessment. A qualitative assessment of the data collected is made from a visual perspective within the area of interest. A data merging is performed using two of the data collection methods to visualize a continuous surface generated from separate data sets. A quantitative assessment of the data collected will be made using statistical tools, specifically Moran's I, Getis-Ord General G statistic calculation and Zonal "Range" statistics, for assessing collection methods. The full analysis process is provided in a block diagram with associated Thesis sections in Figure 13.

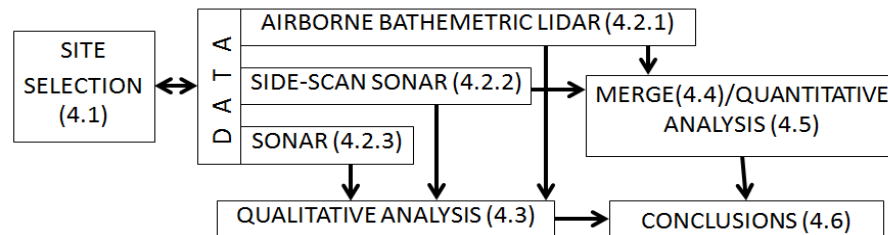


**Figure 13 Block Flow Diagram Outlining Thesis Analysis Process. Numbers in parenthesis indicate section numbers in this chapter.**

#### **4.1 Site Selection**

Initial research to find a suitable location that contains data from all collection methods identified to enable analysis through assessment of the multiple collection methods was difficult. Elements that were sought out in specific were areas that ships regularly utilize as ingress/egress points for transporting goods requiring detailed benthic mapping to navigate safely, areas that have been utilized by ships for a significant length of time that would likely have a significant amount of documented shipwrecks that can be referenced with varying benthic mapping tools for analysis, and areas that have a critical need for benthic mapping that may have source data readily available across a spectrum of benthic mapping tools. Through assessing these key factors Long Island Sound was initially determined to be a suitable location to initiate collection of data for review and analysis in this case study. It should be noted that although extensive research was carried out no ABL data is available for this area.

Long Island is the home of the famous "Wreck Valley" where hundreds of charted wrecks can be found in the waters off Long Island as well as a multitude within Long Island Sound proper inclusive of the USS Ohio and H.M.S. CULLODEN. Although there is extensive Sonar and Side Scan Sonar available, the limitation of ABL availability negated this as the site for analysis. Along the Northeastern Gulf of Mexico and along both east and west shores of Florida there were similar results of one or two of the collected data sets being available but not all three. It became clear that the better

strategy for analysis, if the capability to generate the data sets is not readily available, is to find the data first, then identify the site location based on overlapping data sets

Adopting this strategy, the following core data collection sites were assessed for data collection overlaps: Joint Airborne Lidar Bathymetry Technical Center of Expertise (JALBTCX); U.S. Geological Survey (USGS); and National Oceanic and Atmospheric Administration (NOAA) .

In assessing areas of data overlap between Sonar, Side Scan Sonar and ABL the core data collection sites stipulated several areas of overlap with USGS providing significant SONAR and Side-Scan SONAR for the Rhode Island region JALBTCX was reviewed for ABL data covering the same area. In working through some website challenges coordination with JALBTCX personnel articulated that all data collection has 1km ABL coverage from the shoreline out to sea with comparable land coverage from the shore inland and a direct provisioning covering the area between Watch Hill Point through to Quonochontaug Neck, Rhode Island was provided for analysis. This area is identified in Figure 14 for reference.



**Figure 14 Rhode Island Area of Interest (data developed from ArcMap)**

## 4.2 Data Acquisition

Once data assessments were made and data identified for known overlap areas, the collection of data from core data sites commenced. The USGS, in cooperation with NOAA, is producing detailed geologic maps of the coastal sea floor. Bathymetric Sonar and Side-Scan Sonar data, originally collected by NOAA for charting purposes, provide a fundamental framework for research and management activities, which show the

composition and terrain of the seabed and provide information on sediment transport and benthic habitat. During June 2012, bottom photographs and surficial sediment data were acquired as part of a ground-truth reconnaissance survey of this area. Interpretations were derived from the multi-beam echo sounder, and Side-Scan Sonar, sedimentary, and photographic data collected in Block Island Sound and this outlines the source data that covers the Rhode Island area of interest for Sonar and Side Scan Sonar.

The JALBTCX mission is to perform operations, research, and development in airborne LIDAR bathymetry and complementary technologies to support the coastal mapping and charting requirements of the US Army Corps of Engineers (USACE), the US Naval Meteorology and Oceanography Command, and the NOAA.

The funding to enable data collection by the data groups identified generally comes from the government in Acts or Bills passed such as the American Recovery and Reinvestment Act of 2009, which outlines and provides funding for habitat restoration, navigation projects, vessel maintenance, and other activities. Although there may be funding from private organizations for specific tasking, the majority of the funding is governmental.

#### **4.2.1 USGS Bathymetry Data**

This section of the Thesis is provided by the USGS and defines the collection tools, processing and limitations of the bathymetric SONAR to provide a concept of the amount of hardware and processing required enabling provisioning of the data made available for public consumption. Bathymetric data were acquired in extended Triton data format (XTF) and recorded digitally through TRITON Imaging's ISIS data

acquisition system (TRITON). A RESON SeaBat 7125 multi-beam echo sounder, with a frequency of 400 kHz, was used to collect MBES data with the NOAA ship Thomas Jefferson. All positioning and attitude were determined with Trimble DSM212L DGPS receivers and Applanix POS/MV Model 320 v.4 inertial navigation systems. The data were processed using CARIS Hydrographic Image Processing System (CARIS HIPS) software (CARIS) for quality control, and to incorporate sound velocity and tidal corrections. Sound velocity corrections were derived using frequent SEACAT conductivity-temperature-depth (CTD) profiles (Sea-Bird). Typically, a CTD cast was conducted every three to four hours of multibeam acquisition. Tidal zone corrections were calculated from data acquired at the Newport, Rhode Island, New London, Connecticut, and Montauk, New York tidal gauges. USGS identifies the vertical resolution of the multibeam data is approximately 0.5% of the water depth. Although there are no depth attributes associated with the GeoTIFF image, pixel values convey RGB values of individual cells. Warmer colors (e.g. red) are shallower depths; cooler colors are deeper as shown in Figure 14. The data were gridded to 2-m resolution and saved as a CARIS HIPS database. Vertical datum is mean lower low water; X and Y units are meters; and the projected coordinate system is UTM Zone 19, NAD83. Using CARIS BASE Editor v4.0.5 NOAA data was opened and projected to Geographic (Lat/Lon) WGS84 and then exported to GeoTIFF format (options: Ground Resolution 2m, Image Depth 24 Bit, Background Color White (255,255,255)). Sun illumination was applied from the northeast at 45 degrees above the horizon with a vertical exaggeration of five times to depict the depth information in a shaded relief view.

#### **4.2.2 USGS Side-Scan SONAR Bathymetry Data**

This section of the Thesis is provided by the USGS and defines the collection tools, processing and limitations of the bathymetric Side-Scan SONAR to provide a concept of the amount of hardware and processing required to enable provisioning of the data made available for public consumption. The Side-Scan Sonar data were acquired with a Klein 5000 high-speed Side-Scan SONAR system towed behind one of two 8.5-m aluminum launches deployed from the NOAA ship Thomas Jefferson. The systems consist of a Klein 5500 (Klein, 2015) towfish, a Transceiver/Processing Unit (TPU), and a computer for user interface. The Klein 5000 has an operating frequency of 455 kHz and was set to sweep 100 m to either side of the launch tracks through the formation of five simultaneous, dynamically-focused receiver beams per transducer face. This improves along-track resolution to approximately 20cm at the 100m range scale, even when acquiring data at up to 10 knots. Across-track resolution is typically 7.5cm at the 100m range scale. The achievable 20cm resolution meets the NOAA Hydrographic Surveys Specifications and Deliverables Manual (HSSDM) for object detection. Klein SONARPRO software (Klein) was used to acquire the Klein 5000 Side-Scan sonar data; CARIS SIPS (Side-Scan Image Processing) software was used to process the Side-Scan data and to produce a composite side-scan sonar image at 1-m horizontal resolution and projected into UTM Zone 19 NAD83. The image was imported into Adobe Photoshop CS2 in order to apply a linear stretch of pixel values (i.e., increase the dynamic range of the data), to change the image color space from RGB to 8-bit grayscale, to invert the grayscale to make strong reflections light tones and weak reflections returns darker tones, and to assign a 'NO DATA' value (255). The .tfw file was renamed to match the new

GeoTIFF name and GeoTIFFExamine was used to add the georeferencing information to the TIFF making the image a GeoTIFF.

#### **4.2.3 ABL Data**

This section of the Thesis is provided by JALBTCX and defines the collection tools, processing and limitations of the ABL to provide a concept of the amount of hardware and processing required to enable provisioning of the data made available for public consumption. The ABL data was collected using the Compact Hydrographic Airborne Rapid Total Survey (CHARTS) system (<http://shoals.sam.usace.army.mil/Charts.aspx>) .

The U.S. Army Corps of Engineers collects and maintains LIDAR data including orthophotos in coastal areas of the United States and its territories. The Corps provisioned available data for this Thesis out of data collected from performing its mission of Flood Control, Navigation, Environmental Engineering, and support for the Army and others. Hydrographic data were collected using a SHOALS-1000T flying at 400m altitude, spot spacing 5m x 5m and 1kHz sampling rate. Sensor orientation was measured using a POS AV 410, which measures aerial sensor position and orientation (Applanix).

Prior to survey Position Dilution of Precision (PDOP) was checked and missions planned to avoid PDOP greater than 3.0. During survey the plane was always within 30km of a GPS ground control point, to provide a good quality position solution. Final positions were determined using a post-processed inertially aided Kinematic GPS (KGPS) solution. GPS ground control data were acquired at 1Hz.



Data received by the airborne system were continually monitored for data quality during acquisition operations. Display windows of the collection system showed coverage and information about the system status and center waveforms at 5Hz were shown which allowed the airborne operator to assess the quality of data being collected and the data was processed in the field to verify coverage and data quality.

The SHOALS-1000T data were processed using the SHOALS Ground Control System (GCS). The GCS includes links to Applanix POSPac software for GPS and inertial processing, and IVS Fledermaus software for data visualization, 3D editing, and tie-line analysis. All data were processed in the NAD83 horizontal and vertical datum and later converted to the NAVD88 vertical datum using the GEOID03 model. Fugro in-house utilities were used to split the data into pre-defined boxes, each covering approximately 5km of shoreline. ASCII files of each collection include Longitude, Latitude, UTM Zone, Easting (UTM), Northing, Elevation, Elevation (NAD83), Date, Time and Intensity. The bare earth model was created using Terrascan to define ground points. The ground points were then gridded using Applied Imagery's QT Modeler tool to create a seamless model. The final Bare Earth Model is a 1m resolution GeoTIFF file.

For additional reference points to support quantitative analysis, it is noted that the Office of Coast Survey's Public Wrecks and Obstructions database contains information on the identified submerged wrecks and obstructions within the maritime boundaries of the United States. Information within the database includes the position of each feature (latitude and longitude) along with a brief description. Information to populate the database comes from what is currently available on the electronic navigational chart

(ENC) and OCS's wrecks and obstruction information system. This data was collected as well for reference point assessments and optimal data collection areas.

#### **4.3 Position Accuracy**

Position accuracy of Sonar, Side-Scan Sonar and LIDAR are dependent upon location of the collecting method such as a ship or plane and associated collection tools. Ships and planes use GPS and gyroscope technology to assist in navigation and this also enables positional data to be collected and used in geospatial data collection. In some cases the GPS is separate and the gyroscopes are integrated into an Inertial Navigation System (INS), other systems may have them fully integrated together. The gyroscope tools allow correction of pitch, roll, yaw and altitude during collection and processing the ensure geospatial positioning is accurate.

For bathymetric collections using ABL, SONAR and Side-Scan SONAR all collections utilized the Caris Hydrographic Image Processing System (HIPS) and Side-Scan Image Processing (SIPS) (<http://www.caris.com/products/hips-sips/>), which is a comprehensive hydrographic and SONAR data processing system that enables processing of simultaneous multi beam, backscatter, Side-Scan SONAR, LiDAR and single beam SONAR data. The use of the HIPS and SIPS as a common processing tool for collections provides confidence for increased interoperability within collected and processed products as they are developed by the same company with the same programming language.

As noted previously, Side-Scan SONAR does not provide depth information so it is critical to utilize this technology in conjunction with SONAR and ABL collections to

enable depth measurements such as an associated color band reference during post processing that visualizes elevation for the end user. Side-Scan Sonar has critical use in other areas, such as information about targets on the seafloor, including their position and height above the seafloor, seafloor classification. Side-Scan SONAR frequency can vary from 100kHz to over 1Mhz noting that the higher the frequency, the better your resolution, but the shorter your range scale. USGS collection identifies, the Side-Scan SONAR was collected with a Klein 5000 and has an along-track resolution (direction of ship travel) of approximately 20cm at the 100m range scale, and across-track (perpendicular to ship travel) resolution typically 7.5cm at the 100m range scale with the collection vessel travelling at up to 10 knots. The Klein 5000 system Side-Scan SONAR collection was supported by differential GPS using Trimble DSM212L DGPS receiver with an accuracy of <1m.

The ABL LIDAR data were acquired using a SHOALS-1000T. Prior to survey Position Dilution of Precision (PDOP) was checked and missions planned to avoid a high PDOP, which is the combination of both the Horizontal and Vertical components of position error caused by satellite geometry, of greater than 3.0 (Saylam, 2009). The PDOP accuracy was achieved using the SHOALS Ground Control System (GCS) links to Applanix's POSPac software for GPS and inertial processing. JALBTCX collection identifies the aggregate of the SHOALS-1000T data processing provides horizontal and vertical position accuracy of +/- 3m. It is noted that the +/- 3m accuracy falls within the specification requirements for the data collected and may be improved through utilization of other hardware/software technologies and can be a topic for follow on research. In

review of the SONAR data that was collected, the latitude and longitude accuracy has a resolution of 0.000043 decimal degrees. This data can be re-projected for additional analysis, however, for this Thesis analysis it is maintained in this format as it is the USGS provisioned format for public use. The USGS Digital Elevation Model (DEM) data files are digital representations of cartographic information in a raster form as are the majority of other publically provided data sets. DEMs consist of a sampled array of elevations for a number of ground positions at regularly spaced intervals. These digital cartographic/geographic data files are produced by the U.S. Geological Survey (USGS) as part of the National Mapping Program and the same type of data is collected by States and other government organizations for assessment and processing into the final product which is generally always a raster product for visualization and use. Performing analysis on these products is not intended outside of the accuracy information provided with the data but it can be done through several methods such as collecting the raw data files from initial collection for direct point analysis, reversing the raster process with ESRI tools (e.g. conversion from raster to multipoint) for analysis.

#### **4.4 Qualitative Analysis**

The data collection as identified in the previous section was utilized with ESRI ArcGIS 10.2.2 software for visualization and analysis. The data is raw from what was downloaded or provided via the core data providers identified and no additional configuration of the data was done to improve visualization.

The selected area south of Quonochontaug, RI provides unique bathymetric structural images as well as cavernous mountainous regions that have sharp contrast and allow for excellent visualization and assessment within the data sets collected. The figures within this section identify the imagery attained from Sonar, Side-Scan Sonar and ABL at similar scales with associated analysis.

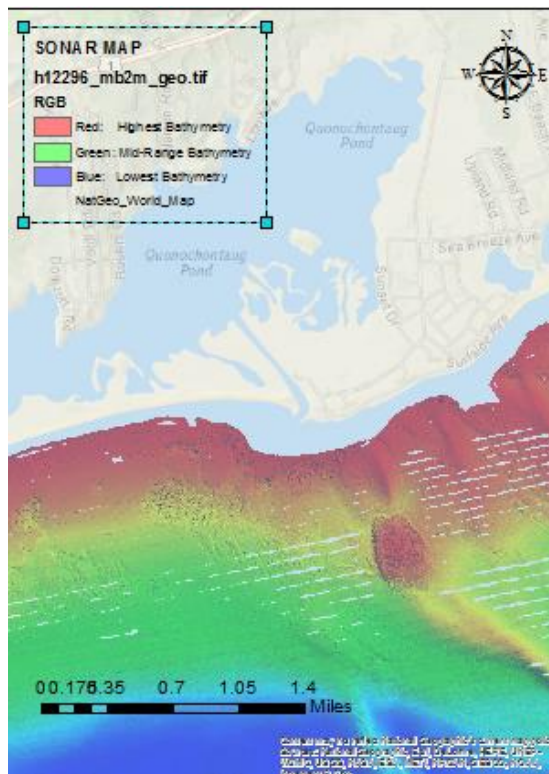


**Figure 15 Sonar Data Visualization; Rhode Island**

As can be seen in Figure 15, for Sonar data visualized at 1:25000 there are visible contours and depths that can be measured readily within the tools used to visualize the

data. Each of the data sets (Sonar, Side-Scan Sonar and ABL) originates in point cloud data and the visualization is an interpolation of that point cloud data to the user's needs. With the above Sonar the clarity and the functionality for visual analysis is aesthetically of a higher value than with the same scale visualization of the Side-Scan Sonar and ABL data. It is of note that this data is collected at a frequency of 400 kHz and gridded to 2 meter resolution.

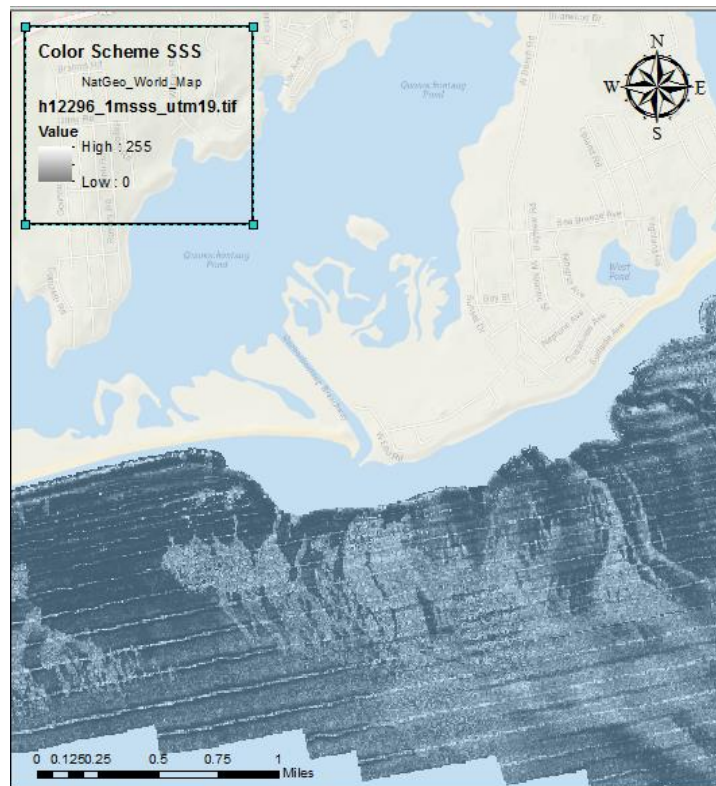


**Figure 16 Side-Scan Sonar Data Visualization; Rhode Island**



In Figure 17, visualizing the ABL data at 1:25000 it shows visible contours and depths that can be measured readily within the tools used to visualize the data. This data is less comparable with the Sonar imagery and Side-Scan Sonar imagery at this scale and, although it provides visualization of the area with associated depths and contours, it is less effective for visual assessments and lacks the visual depth that the Sonar and Side-Scan Sonar provides. The data visualization at this scale provides tracking of higher level detail (large scale images, footprints and overall depth), which can be utilized for bathymetric assessment, however, it has less visualization assessment value than Sonar and Side-Scan Sonar as the peaks and valleys less comparable between the other data collection imagery provided at the same zoom level. It is of note that this data is collected at a frequency of 1 kHz and gridded to 1m resolution.

To further explore what the data can visually offer at different scales, another assessment was made using the same data and assessing the region to the lower left and lower right of the Quonochontaug Pond inlet. The data set clips provide SONAR over a vertical range of 250m, ABL over a vertical range 30.45m and Side-Scan SONAR over a vertical range 254m (noting that Side-Scan SONAR does not provide a z value when collected). Two separate two data frames were provided for visualization purposes of each data set with red and white outlines for each data frame correlating to red and white extent indicators for clarity and emphasis on the identical assessment regions that contain distinct topography.



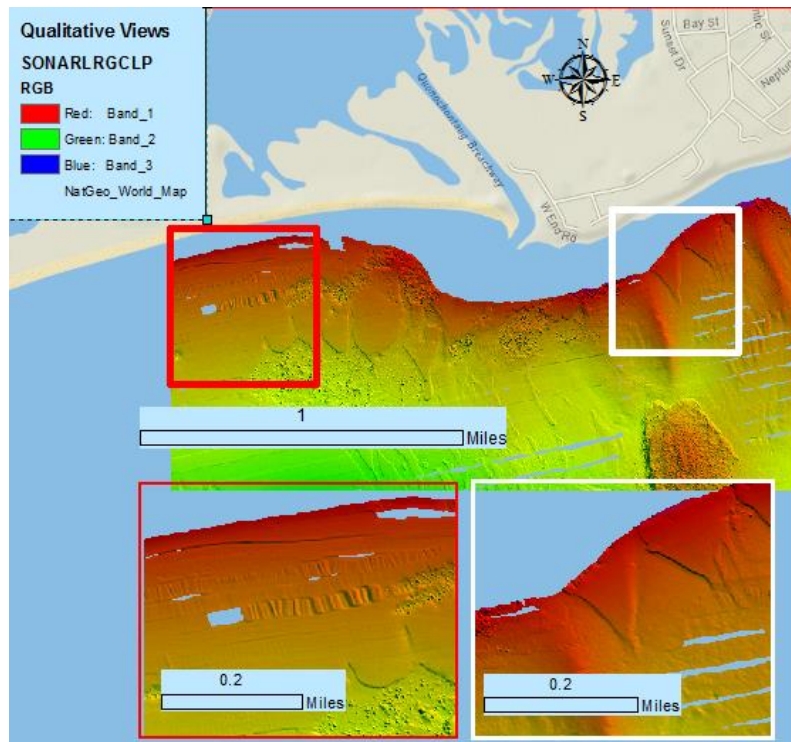


**Figure 18 Sonar data visualization, Rhode Island case study area; In this figure depth values are visualized by color, from low depth (dark red) to high depth (dark blue)**

As can be seen in Figure 18, the Sonar data visualized at two tenths of a mile provides visible contours and shapes that can be measured readily within the tools used to visualize the data. Again, with the above Sonar data, the clarity and the functionality for visual analysis is of higher value than with the visualization same scale of the Side-Scan Sonar and ABL data.

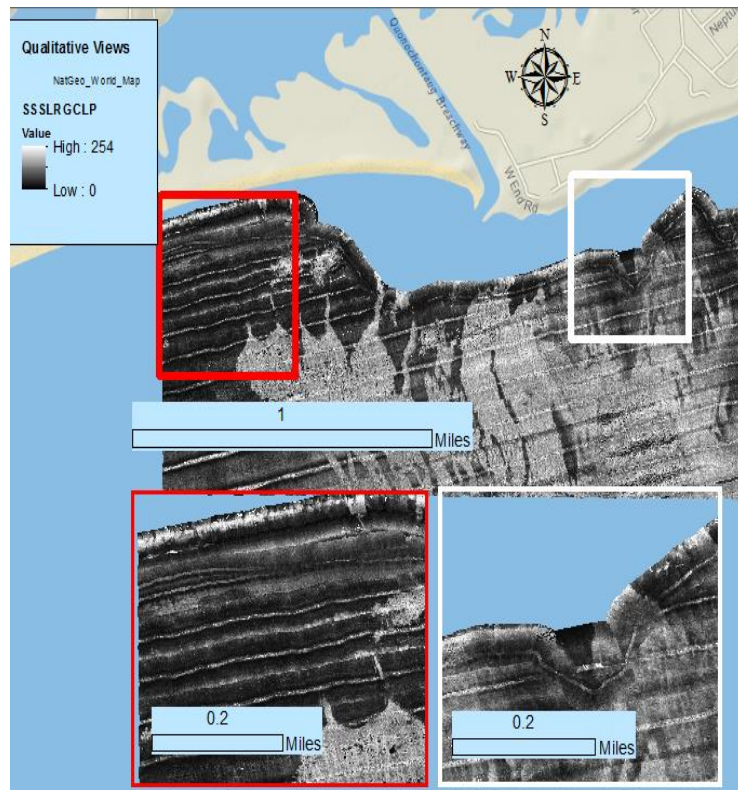


**Figure 19 Side-Scan Sonar Data Zoom Visualization; Rhode Island; In this figure depth values are visualized by grey level values, from low depth (white) to high depth (black)**

As can be seen in Figure 19 for Side-Scan SONAR data visualized at two tenths of a mile, the contours, depths and shapes are less noticeable at this scale although when used in conjunction with SONAR collections they yield comparable depth measurements within the tools used to visualize the data. At higher resolution the Side-Scan SONAR imagery has less visual analysis value than SONAR based on the lessened ability to clearly visualize the peaks and valleys but, although limited, has more qualitative value than the ABL collection at this scale.

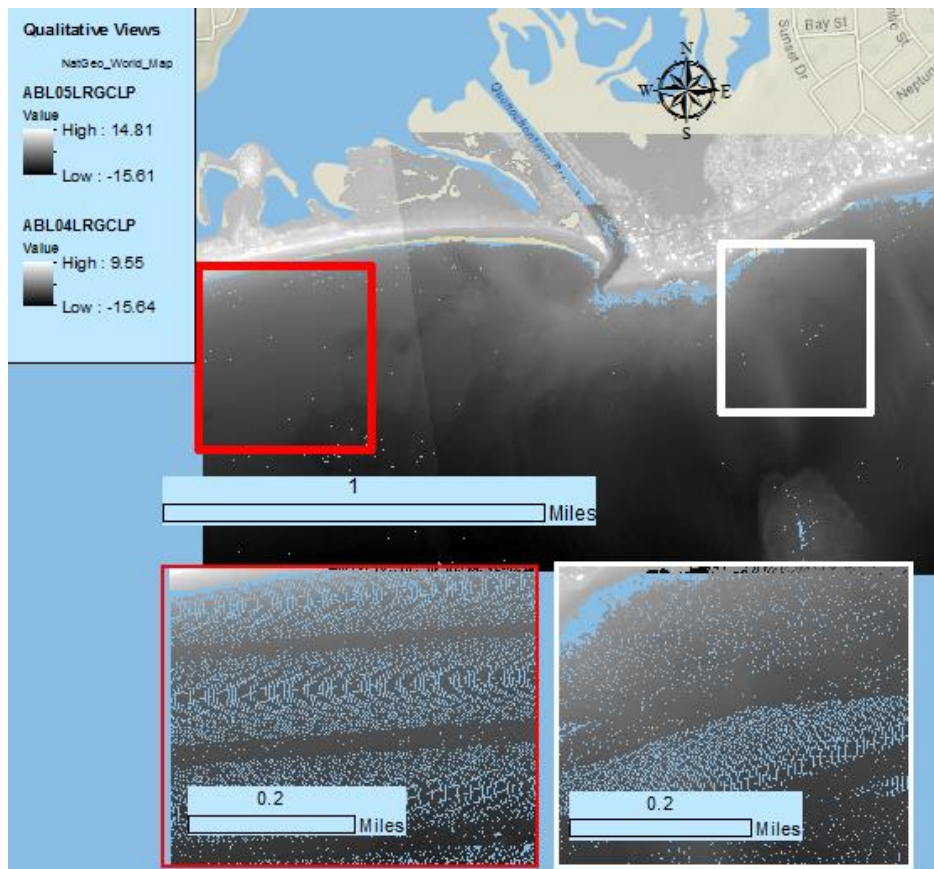


**Figure 20 ABL Data Zoom Visualization; Rhode Island; Legend values are in meters and there are two color scale bars as there are two data sets side by side in this figure**

As can be seen in Figure 20 for ABL data visualized at two tenths of a mile, the contours, depths and shapes are not noticeable at this scale although when used in conjunction with SONAR they yield roughly the same depth measurements within the tools used to visualize the data. With the data collected and at higher resolution, the imagery has no qualitative visual analysis value because of the pixilation incurred, unless it is used in conjunction with other data such as SONAR or Side-Scan SONAR. The

side-by-side view of the qualitative imagery between SONAR, Side-Scan SONAR and ABL is provided in Figure 21 for reference.

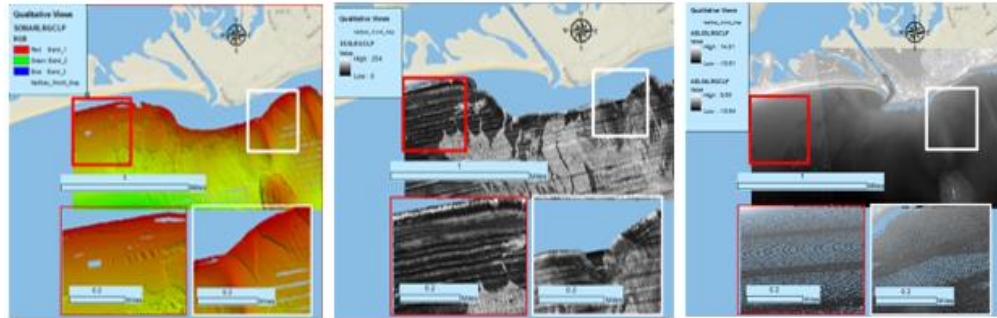


**Figure 21 SONAR, Side-Scan SONAR and ABL Data Zoom; Rhode Island**

One additional image was collected for an understanding of the visualization capacity that the SONAR data in conjunction with the Public Wrecks and Obstruction data. For this image scanning the Public Wrecks and Obstruction data and SONAR data only led to an optimal image 800 meters south of Watch Hill Light in Westerly, RI (southernmost point of Rhode Island) and what is depicted of what was thought to be available from the other collected data sets. Figure 22 outlines two sunken ship wrecks – the red is a sunken ship that poses a hazard to vessels and the blue is a sunken ship that is well below the murky depths and poses no risk to any floating vessels.

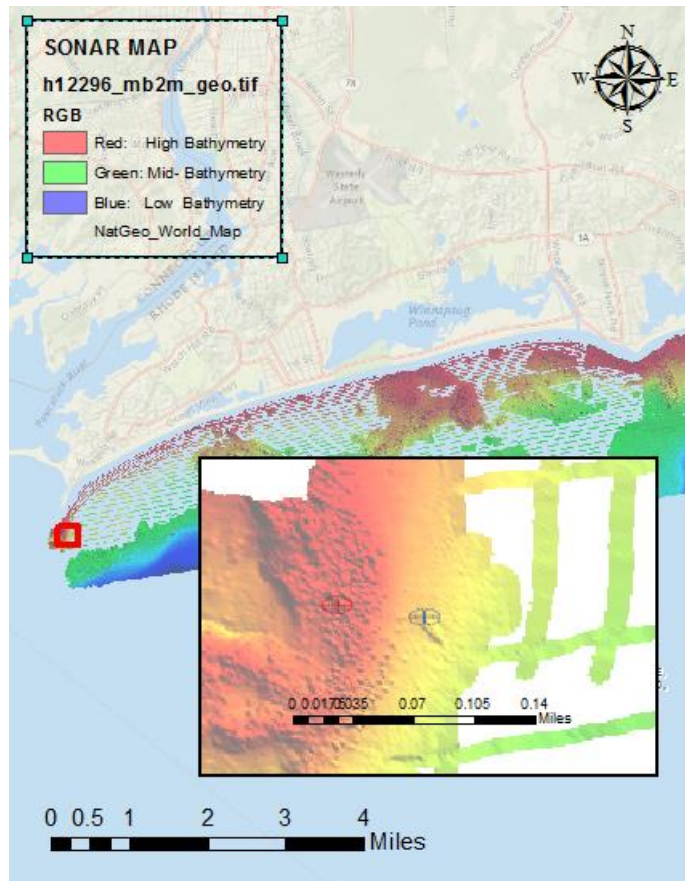


**Figure 22 Sonar Data with Wrecks Zoom to Ship (1:3889); Rhode Island**

The pixilation effect of the red ship is not as noticeable as it may be a smaller sunken vessel; however there is no ambiguity of the “blue” marked wreck. Of note are the strips on the right of the image, these are areas lack data and are “null” from the original data collection.

#### **4.5 Data Merge Analysis**

Due to increasing availability and easier access to DEMs at a broad range of spatial resolutions (from LiDAR at several centimeters up to GTOPO30, the global 30 arc



second digital elevation model project, at approx. 1 km), multi-scale analysis of the land and bathymetric surfaces are becoming more feasible. The modeling of scale effects with respect to both changing resolution and varying window size for surface calculations has been identified as a major research topic not only in geomorphometry, but rather in all disciplines dealing with DEMs including hydrology, soil science, and geomorphology. (Lucian Drăgut, 2011)

Though merging data sets that have the same resolution and projection would be ideal, this may not always be easy to accomplish. If one has original source data that is in different projections, potentially different vertical datums (e.g. Mean Sea Level or WGS84) and even diverse data formats the data sets ideally would be converted into similar projections, datums and formats. Current geospatial tools support these conversions and, through simple conversion steps of various data collections, can allow merging of dissimilar data.

An approach to merging DEMs could include the following steps: Interpolation into a common projection, determining grid spacing for algorithm analysis, development of an algorithm to assess the grid spacing of overlapping data with associated criteria (e.g. averaging of elevation within the respective grid), data integration into a merged product and then follow on analysis on the resulting DEM for accuracies. (Hongxing Liu, 1999). This approach is one of many that can be utilized and the variances and resulting DEM integration approaches are a field of study that requires additional research to fully appreciate but the outlined approach provides the reader with an

understanding of one methodology and the knowledge there are multiple variables that would need significant attention when merging DEMs.

Through the creation of a Mosaic using the raster data set tools, two of the ABL data collections and the Side-Scan SONAR for this Thesis were merged. The data from one of the ABL files was selected as the target data set and the Side-Scan Sonar was re-projected to the baseline (target) coordinate system with the overlapping area blended by taking the mean of the overlapping cell values resulting in one Mosaic product which provides a continuous plan from the ABL land collection, the ABL/Side-Scan Sonar overlap, where the mean value is calculated which is displayed as hill shaded and visualized in Figure 23.



**Figure 23 Image Generated from Mosaic of Side-Scan Sonar and ABL; Rhode Island; In this figure depth values are visualized by grey level values, from low depth (White) to high depth (Black)**

The hill shade effect on the mosaic data merge provides a good visualization using the mosaic tools that are available in ESRI 10.2.2. Additional functionalities available in ESRI 10.2.2 release which provides a toolbox tool “Production Contouring” that contains a “Merge and Filter” selection allowing Digital Elevation Models to be merged directly, filtered directly, or merged and filtered with selections that the user wishes to incorporate. Fundamentally, the ability to join data sets has been seen as a need and the commercial industry is adapting to this need by providing additional tools that enable the user to meet these needs. The merged image provided does provide



confirmation of the ability to merge data sets and can be used to link the historic land DEM data and Bathymetric DEM data.

## 4.6 Quantitative Analysis

To assess the data further using quantitative analysis, the spatial autocorrelation (specifically Global Moran's  $I$ ) was used which is an inferential statistic, meaning that the results of the analysis are always interpreted within the context of its null hypothesis. The most often used and cited spatial autocorrelation tool is Moran's  $I$ , a single test statistic that indicates two types of spatial autocorrelation—positive autocorrelation and negative autocorrelation with outputs of an associated p-value,  $I$  value and z-value which allow one to assess if the data that is on hand is spatially autocorrelated randomly (very low p-value ) the amount of spatial autocorrelation (if the  $I$  value is close to zero) or if there is an underlying spatial process at work that either leans towards more spatial clustering (Positive z-value) or towards spatial dispersion (Negative z-values) (deSmith, Goodchild, & Longley, 2015). These two autocorrelation indicators, positive and negative, have been used widely to capture three types of spatial relations: a positive autocorrelation captures the existence of both high-value clustering and low-value clustering, while a negative autocorrelation captures the juxtaposition of high-values next to low-values (Zhang & Ge, 2007). For the Global Moran's  $I$  statistic, the null hypothesis states that the attribute being analyzed is randomly distributed among the features in your study area. The Global Moran's  $I$  provides the Moran's  $I$  Index, Expected Index, Variance, z-score, and p-

value. The p-value is the probability that the observed spatial pattern was created by some random process. When the p-value is very small, it means it is very small probability that the observed spatial pattern is the result of random processes, so you can reject the null hypothesis. Z-scores are a measurement of standard deviation where, if you had a output value of 1.5, the result would be that the z-score is 1.5 standard deviations. Very high or very low (negative) z-scores, associated with very small p-values, are found in the tails of the normal distribution (ESRI, 2015). Z-scores and p-values are associated with the standard normal distribution in Figure 24 and Table 2 summarizes the interpretation of p-value and z-score results.

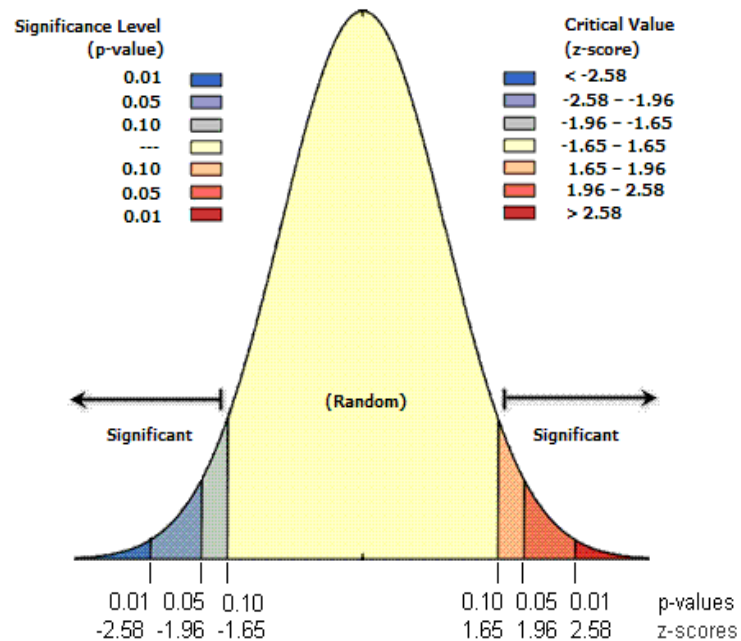


**Figure 24 Z-scores and P-values associated with the standard normal distribution (ESRI, 2015)**

**Table 2 Interpretation of Moran's I Output (ESRI, 2015)**

The p-value is <i>not</i> statistically significant.	You cannot reject the null hypothesis. It is quite possible that the spatial distribution of feature values is the result of random spatial processes. The observed spatial pattern of feature values could very well be one of many, many possible versions of complete spatial randomness (CSR).
The p-value <i>is</i> statistically significant, and the z-score is positive.	You may reject the null hypothesis. The spatial distribution of high values and/or low values in the dataset is more spatially clustered than would be expected if underlying spatial processes were random.
The p-value <i>is</i> statistically significant, and the z-score is negative.	You may reject the null hypothesis. The spatial distribution of high values and low values in the dataset is more spatially dispersed than would be expected if underlying spatial processes were random. A dispersed spatial pattern often reflects some type of competitive process—a feature with a high value repels other features with high values; similarly, a feature with a low value repels other features with low values.

The Global Moran's I tool was applied to the collected data sets for assessing spatial autocorrelation. The tool calculates spatial autocorrelation based on feature locations and feature values simultaneously to evaluate whether the pattern expressed is clustered, dispersed, or random (ESRI, 2015). In preparation for this analysis all data sets were projected to WGS 1984 UTM Zone 19N, clipped to a region roughly 1300m by 1660m (removing areas with no data) within the previously identified area of interest, and converted from raster data sets to point feature geometry to ensure data commonality for

assessment. The calculation formulas that are used to provide the Spatial Autocorrelation assessment are identified in Figure 25 for reference.

The Moran's  $I$  statistic for spatial autocorrelation is given as:

$$I = \frac{n}{S_0} \frac{\sum_{i=1}^n \sum_{j=1}^n w_{i,j} z_i z_j}{\sum_{i=1}^n z_i^2} \quad (1)$$

where  $z_i$  is the deviation of an attribute for feature  $i$  from its mean ( $x_i - \bar{X}$ ),  $w_{i,j}$  is the spatial weight between feature  $i$  and  $j$ ,  $n$  is equal to the total number of features, and  $S_0$  is the aggregate of all the spatial weights:

$$S_0 = \sum_{i=1}^n \sum_{j=1}^n w_{i,j} \quad (2)$$

The  $z_I$ -score for the statistic is computed as:

$$z_I = \frac{I - E[I]}{\sqrt{V[I]}} \quad (3)$$

where:

$$E[I] = -1/(n - 1) \quad (4)$$

$$V[I] = E[I^2] - E[I]^2 \quad (5)$$

**Figure 25 Moran's I Calculations (ESRI, 2015)**

Figures 26, 27, and 28 provide the Global Moran's I assessment of SONAR, Side-Scan SONAR and ABL respectively with the Spatial Autocorrelation tool returning the

associated output values of the Moran's I Index, Expected Index, Variance, z-score, and p-value for each assessed data set.

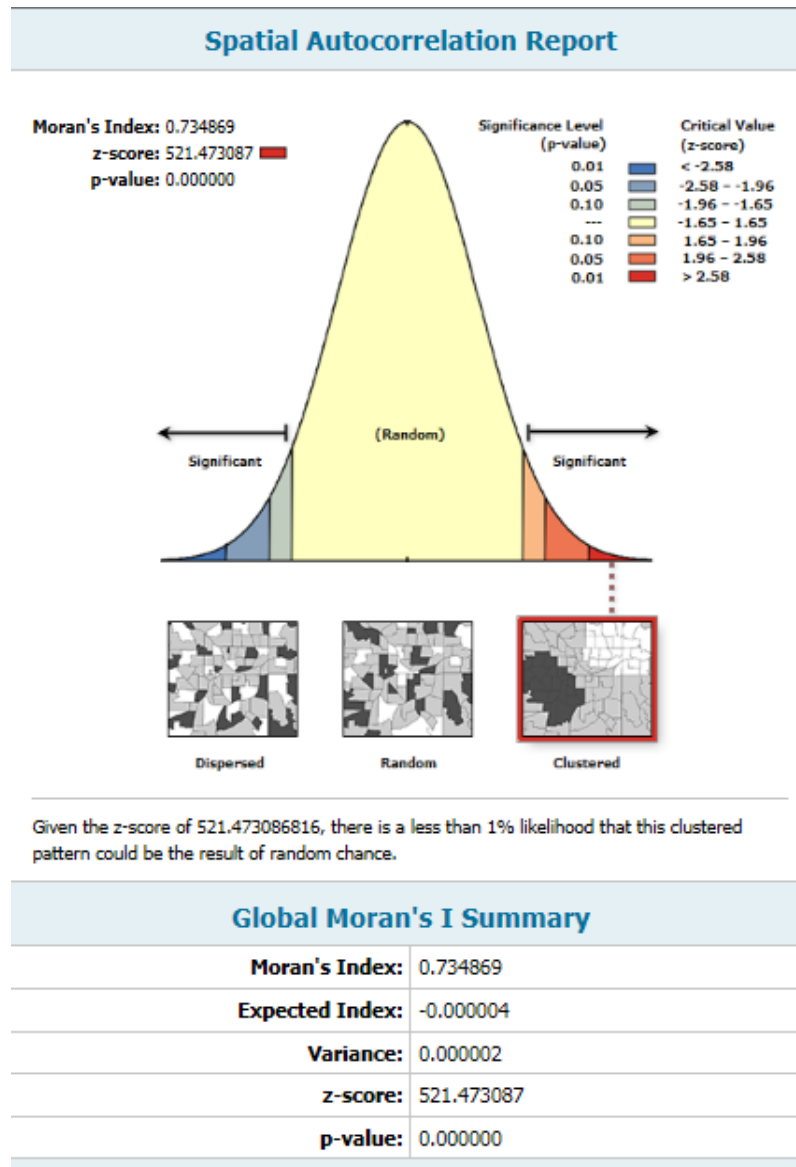


**Figure 26 Moran's I Executed on SONAR (ArcGIS 10.2.2)**

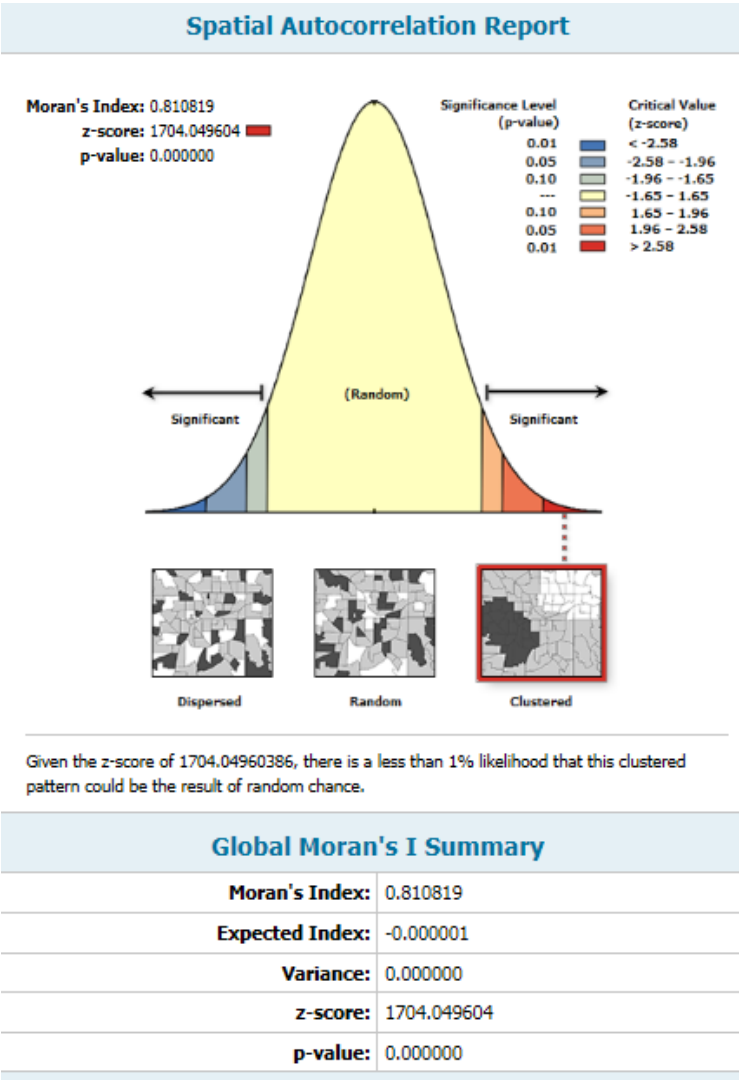


**Figure 27 Moran's I Executed on Side-Scan SONAR (ArcGIS 10.2.2)**

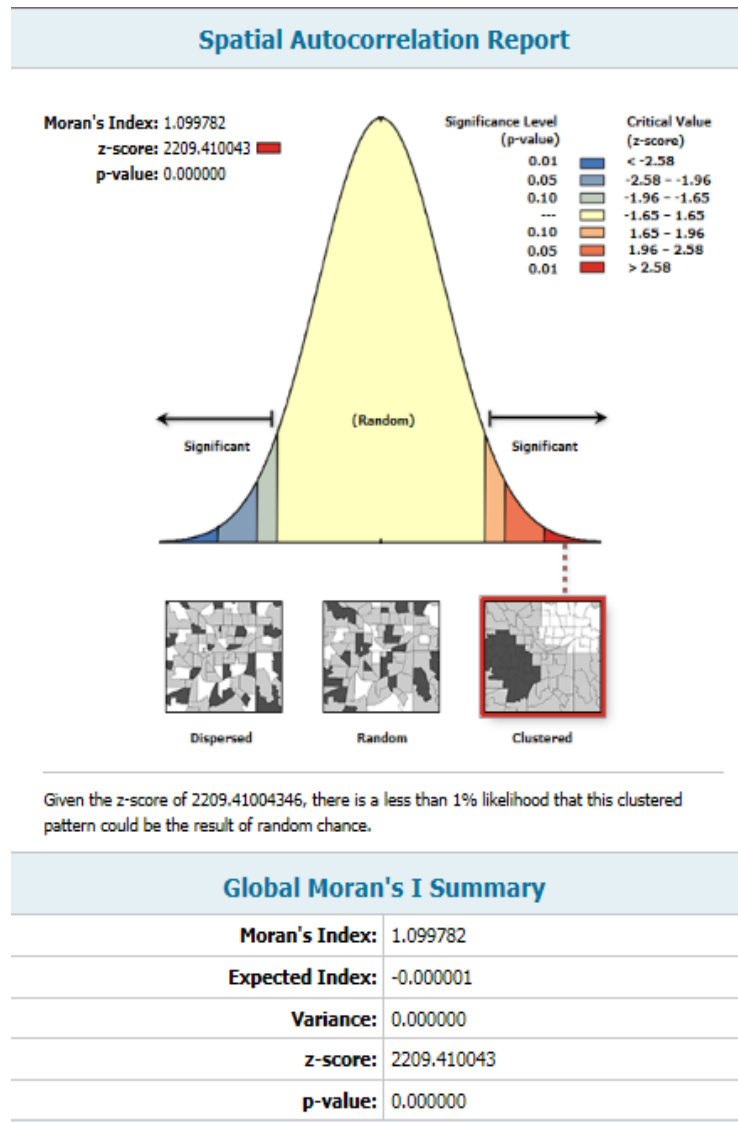


**Figure 28 Moran's I Executed on ABL (ArcGIS 10.2.2)**

With each of the Moran's I test executions for the associated data sets the p-values were essentially zero and the z-score was positive in all cases. The results across all assessments with Moran's I provides values allowing rejection of the null hypothesis and articulation that the spatial distribution of high values and/or low values in the dataset

is more spatially clustered than would be expected if underlying spatial processes were random which, from a geospatial perspective, shows some evidence that there is some underlying spatial process at work.

As an additional step for quantitative analysis the Getis-Ord General G statistic was calculated using the High/Low Clustering tool within ArcGIS 10.2.2 in order to measure the degree of clustering for either high values or low values within the data sets. As the input field for this tool cannot have negative numbers (e.g. ABL cannot be used as it has negative values in the regions that cover bathymetry) only the SONAR and Side-Scan SONAR data sets were assessed with an output of G: 0.000009, z-score: 207.1704, p-value: 0.0000 and G: 0.00011, z-score: 649.4958, p-value: 0.0000 respectively. As with the results from Moran's I, the p-values allow dismissal of the null hypothesis, which is the same for both tools, and with respect to the General G z-value positive/negative values correlate to the spatial distribution of high/low values, respectively, in the dataset being more spatially clustered than would be expected if underlying spatial processes were truly random (ESRI, 2015). The calculation formulas that are used to provide the Getis-Ord General G assessment are identified in Figure 29 for reference.



The General G statistic of overall spatial association is given as:

$$G = \frac{\sum_{i=1}^n \sum_{j=1}^n w_{i,j} x_i x_j}{\sum_{i=1}^n \sum_{j=1}^n x_i x_j}, \quad \forall j \neq i \quad (1)$$

where  $x_i$  and  $x_j$  are attribute values for features  $i$  and  $j$ , and  $w_{i,j}$  is the spatial weight between feature  $i$  and  $j$ .  $n$  is the number of features in the dataset and  $\forall j \neq i$  indicates that features  $i$  and  $j$  cannot be the same feature.

The  $z_G$ -score for the statistic is computed as:

$$z_G = \frac{G - E[G]}{\sqrt{V[G]}} \quad (2)$$

where:

$$E[G] = \frac{\sum_{i=1}^n \sum_{j=1}^n w_{i,j}}{n(n-1)}, \quad \forall j \neq i \quad (3)$$

$$V[G] = E[G^2] - E[G]^2 \quad (4)$$

**Figure 29 Getis-Ord General G Calculations (ESRI, 2015)**

To provide clarification of what the Moran's I and Getis-Ord General G statistic assessed the Hot Spot Analysis with Rendering tool was used on the SONAR data for visualization. The tool calculates the Getis-Ord  $G_i^*$  statistic for hot spot analysis and then applies a cold-to-hot type of rendering to the output z-scores where the blue areas signify low level clustering and the red areas signify high level clustering. Figure 30 identifies the calculations for the  $G_i^*$  statistic.

The Getis-Ord local statistic is given as:

$$G_i^* = \frac{\sum_{j=1}^n w_{i,j} x_j - \bar{X} \sum_{j=1}^n w_{i,j}}{S \sqrt{\frac{n \sum_{j=1}^n w_{i,j}^2 - \left( \sum_{j=1}^n w_{i,j} \right)^2}{n-1}}} \quad (1)$$

where  $x_j$  is the attribute value for feature  $j$ ,  $w_{i,j}$  is the spatial weight between feature  $i$  and  $j$ ,  $n$  is equal to the total number of features and:

$$\bar{X} = \frac{\sum_{j=1}^n x_j}{n} \quad (2)$$

$$S = \sqrt{\frac{\sum_{j=1}^n x_j^2}{n} - (\bar{X})^2} \quad (3)$$

The  $G_i^*$  statistic is a z-score so no further calculations are required.

**Figure 30 Getis-Ord Gi\* Calculations (ESRI, 2015)**

The Getis-Ord Gi\* complements the Getis-Ord General G in that it provides visualization of the z values in the regions that the General G z-value identifies as spatially autocorrelated. As both the Moran's I and Getis-Ord General G statistic analysis pointed out, this clustering is not random and was created by some underlying spatial process which can be seen in the contours of the image in Figure 31 which is the output of Getis-Ord Gi\* execution.

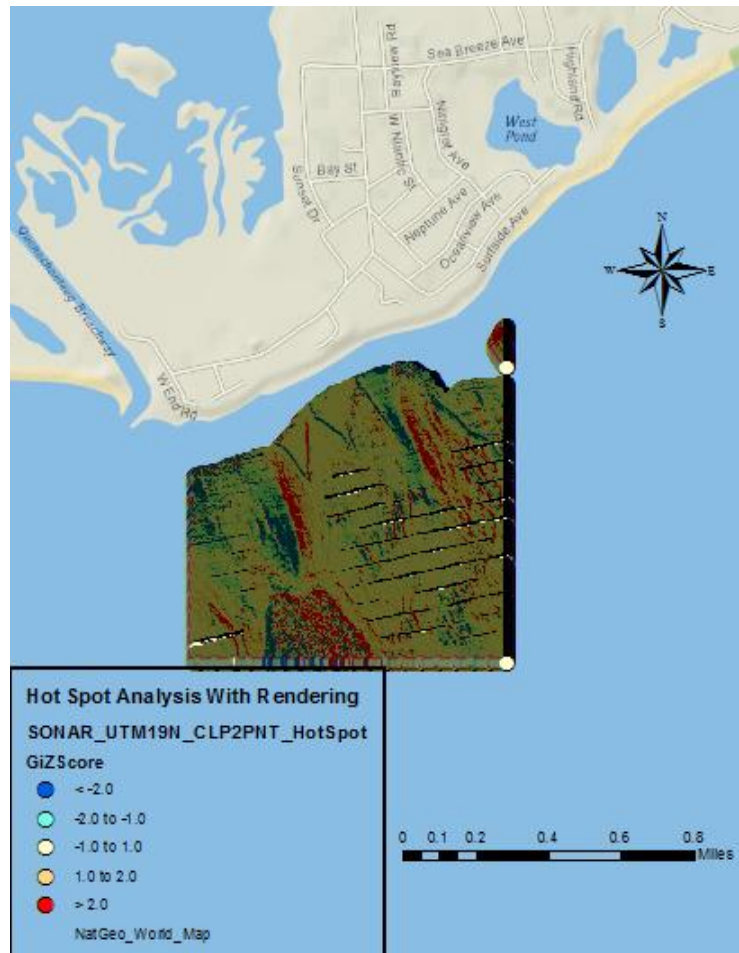


**Figure 31 SONAR Hot Spot Analysis with Rendering (ArcGIS 10.2.2)**

One further step to provide a quantitative assessment was to execute Zonal statistics on the SONAR and the ABL data sets. With the zonal statistic tools, a statistic is calculated for each zone defined by a zone dataset, based on values from another dataset (a value raster and a single output value is computed for every zone in the input zone dataset).

A zone is all the cells in a raster that have the same value, whether or not they are contiguous. The input zone layer defines the shape, values, and locations of the zones, an integer field in the zone input is specified to define the zones and a string field can also be used to support analysis. One thing to note with zonal analysis is that both raster and feature datasets can be used as the zone dataset. The input value raster contains the input values used in calculating the output statistic for each zone (ESRI, 2015).

The Zone layer demonstrates an input raster that defines the zones, the Value layer contains the input for which a statistic is to be calculated per zone and, as Figure 32 articulates, the maximum of the value input is identified for each zone.

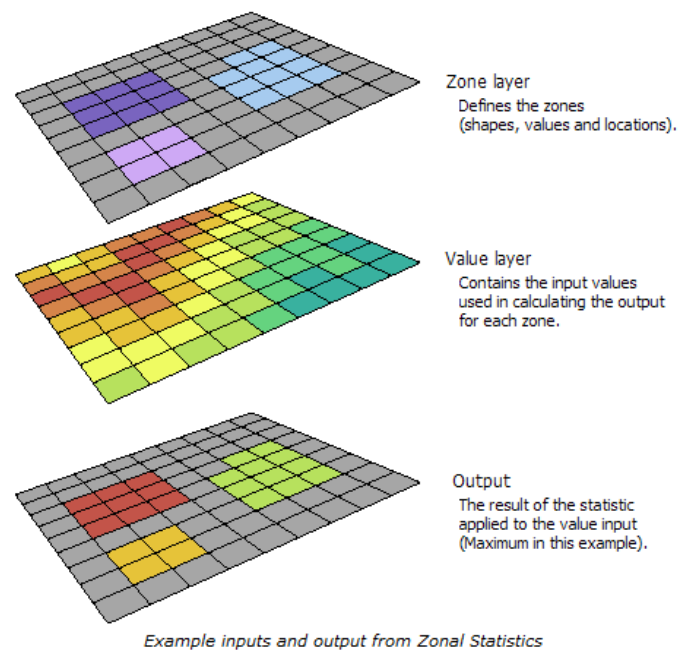


**Figure 32 Example Inputs and Output from Zonal Statistics (ESRI, 2015)**

The same data sets that were used for Moran's I and Getis-Ord General G statistic analysis were used for Zonal analysis with the SONAR data set being the input raster, the value field was selected as the Zone field and the ABL data was selected as the input value raster. The statistical type of analysis selected was "Range", which calculates the difference between the largest and smallest value of all cells in the value raster that belong to the same zone as the output cell.

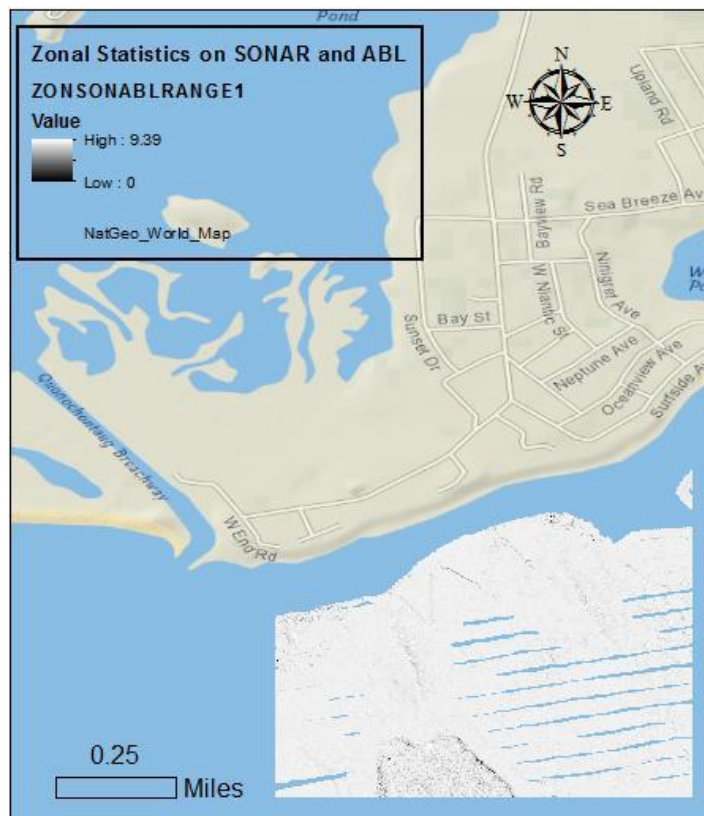


**Figure 33 Example Inputs and Output from Zonal Statistics; Legend measurements are in meters**

Execution of the Range Zonal analysis with the expected outcome of the area where the SONAR and ABL overlapped with associated values was obtained and is shown in Figure 33. This output denotes that there are regions where there are differences between the z values of the two data sets assessed of up to 9.39m. To review what appears to be a systematic difference in the Range Zonal analysis (the image in Figure 33 being primarily white) the raster was converted to a point features and normalized using the following formula:  $((\text{data} - \text{mean}) / \text{Standard Deviation})$  and execution of Moran's I on that output was completed and shown in Figure 34. The results of Moran's I provided a p-value = 0.0000 and a z-value = 318.0126 which, again, allows rejection of the null hypothesis and articulation that the spatial distribution of high values and/or low values in the dataset is more spatially clustered than would be expected if underlying spatial processes were random leading to the theory that the spatial difference visualized may be systematic from either data collection methods or processing.

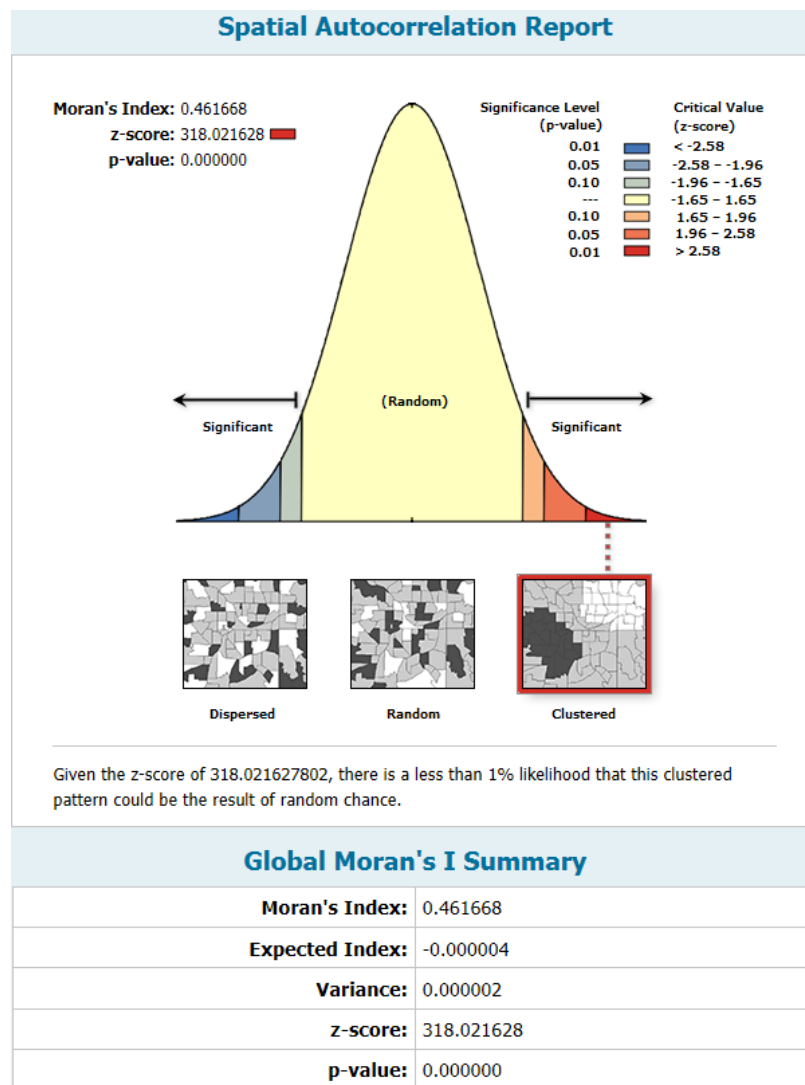


**Figure 34 Moran's I Executed on Range Zonal Analysis (ArcGIS 10.2.2)**

With the qualitative data captured in this section there is a high level of confidence in the data sets that were attained and in that these data sets can be used for the purposes of boating/shipping and Green Energy wave energy converter technology inputs. In any regions where there is concern of safety based on the Range Zonal analysis it is recommended that additional verification through bathymetric ground truth analysis.

## **CHAPTER 5: CONCLUSIONS**

Bathymetry has traditionally been performed using echo sounders (sonars) mounted on ships or boats. Over time the development and use of multi-beam echo sounders has allowed for highly detailed, accurate seabed charting. While these systems can measure depths even in shallow water, boats cannot access areas that are rocky, have shallow reefs, have long shallow beaches and areas that incur large waves. Additionally, echo sounder systems are expensive and difficult to deploy at short notice.

In order to penetrate the denser medium of water and then minimize scattering, LIDAR bathymetry requires much higher power and longer laser pulses than topographic LIDAR. Therefore, bathymetric systems operate at a much slower rate and with much longer pulses than topographic ones. For example, a new system that JALBTCX is working on is a \$13 million, 5 year effort for the U.S. Army Corps of Engineers to develop a new sensor for mapping and charting coastal zones called Optech's Coastal Zone Mapping and Imaging Lidar (CZMIL) which has a measurement rate of 70 kHz when operating in topographic mode but of only 10 kHz when operating in hydrographic mode. Additions to the data collection approach with this 5 year effort will include seamless bathy/topo Digital Elevation Models (DEMs), bare earth DEMs, shoreline vectors and RGB and hyperspectral orthomosaics to assess both land and bathymetry (Dodd & Barbor, 2013).



The critical point within the ABL collection is the lower pulse frequency which reduces the achievable point density, which impacts smaller resolution capacities.

Additional concerns with airborne collection is that even in relatively smooth air, all aircraft are subject to vibrations, sudden loss of attitude, and constant small changes in their pitch, roll and yaw. Therefore, knowing the range to a target alone, such as laser return time, is not sufficient to determine its position, which also requires knowledge of the aircraft's exact location and attitude at the time each laser pulse is fired. Differential GPS provides the former and an inertial measurement unit (IMU) provides the latter. Overall the ABL systems make it possible to quickly survey, in a single scan, features and constructions both above and below the waterline and, typically, digital images are recorded at the same time, enabling their visual analysis and use with digital terrain models which is the significant capability.

From an initial review it was apparent that the ABL data would be significantly better in determining underwater objects within 1km from the shoreline. In assessing the resolution, the ABL data provided begins to significantly pixilate when zooming in beyond 1:25000 scale, a factor of the lower frequency rate which impacts higher resolution and visualization of collections. In land mapping, detail available at the 1:25,000 scale generally includes minor paths, field boundaries and open access areas. The assumption was that visualization of smaller underwater structures would be feasible at this resolution and identify a cost effective research tool for such applications – this is not fully the case and review of the data for application purposes is necessary to understand these limitations.

The previously held perception that ABL is a better geospatial tool for shipping and ECW application analysis is proven inaccurate with the data collected and assessed. The Sonar capabilities for fine resolution far outperform the current ABL capabilities; however, for larger scale concerns that can be addressed at the 1:25000 scale, all collection capabilities reviewed in this thesis have merit. For applications that require higher scale resolution than 1:25000 in shallow bathymetric areas there is still a gap that the developing CZMIL system may be able to fill in the near future. The data that was collected and analyzed covered roughly one square mile and, with sound engineering judgment, can be correlated to other bathymetric regions data collections.

Just as the progression from lead lines to Sonar came to fruition and then from Sonar to multi-band Sonar and expansion into Side-Scan Sonar progress came. Now, with a decade of LIDAR coming into play and expanding the capabilities of remote sensing decreasing time and, possibly cost with increasingly accurate and useful multifunctional data to combine with past data collections there is more progress. In the time to come there will be additional technological advancements that will fill gaps and enable more efficient and effective remote data collection... it is just a matter of time.

## **5.1 Discussion**

For the purposes of supporting boating and shipping transportation with bathymetry within roughly 1km of the shoreline ABL may not be the preferred tool at this time based on the data collected for this Thesis. The capacity of ABL being a faster, more economic method to collect data can bring this tool to the forefront for use. A

multitude of applications will turn to ABL as the preferred tool based on these factors and use will grow over time and as advancements in ABL scanning, collection and processing techniques come into play. As discussed in the previous section, CZMIL is a tool that has significant funding to support better ABL collections and should be assessed when the project comes to completion as a follow on effort. Even as there is testing to utilize alternate methods to tow Side-Scan SONAR “fish” to reduce risk, time and costs for data collection may become a very effective approach to attaining higher resolution shallow water bathymetry. In the short term, there are solid Sonar and Side-Scan Sonar collection capabilities that will enable the more finite assessment needs that exist in safe, deeper water and a growing utility with the ABL that is current and becoming available.

The second component that led to the initiation of the bathymetric analysis tools in this thesis was Marine renewable energy. Marine renewable energy generally consists of wave energy and offshore wind which are exciting recent green energy approaches. With initial interest in green energy and reading into Marine renewable energy, the engineering questions began to enter the thought process on how and where the ideal placement of these devices could be identified. Additional research on benthic data collection methods and tools is required which lead to the research and development of this Thesis.

Through assessing Sonar, Side-Scan SONAR and LIDAR tools it is apparent that all of them can be utilized to engage the Marine renewable energy fields and provide data that would be critical to the analysis and placement of wave energy devices as well as offshore wind devices. The advent of hyperspectral imagery within the ABL data

collections coming into play would add additional vegetation / sediment data that could identify bedrock locations that may be ideal for the placement of Marine renewable technologies.

One such Marine renewable energy technology would be the Oyster Wave Energy Converter (WEC). The Oyster WEC comprises an Oscillator flap mounted on a Sub-frame Support Structure. The oscillating action of waves on the flap drives hydraulic pistons, which pressurize seawater. The pressurized seawater is pumped to shore through high pressure pipelines. At shore the hydroelectric plant converts the hydraulic pressure into electrical power via a pelton wheel, which turns the electrical generator. The device is located at depths between 10m and 15m at a distance from shore of around one half km. The flap is 18 m wide by 11 m high and secured to the sea bed by drilled and grouted piles in a connector frame. (L. Cameron, 2010) Use of ABL hyperspectral data could quickly and cost effectively identify bedrock or ideal placement areas that may support potential site designations to choose from for the placement of these devices. The Oyster WEC is only one technology and there are over 1000 WEC techniques that have been patented in Japan, North America and Europe. (Clément, 2009) Figure 35 outlines the Oyster WEC technological approach.

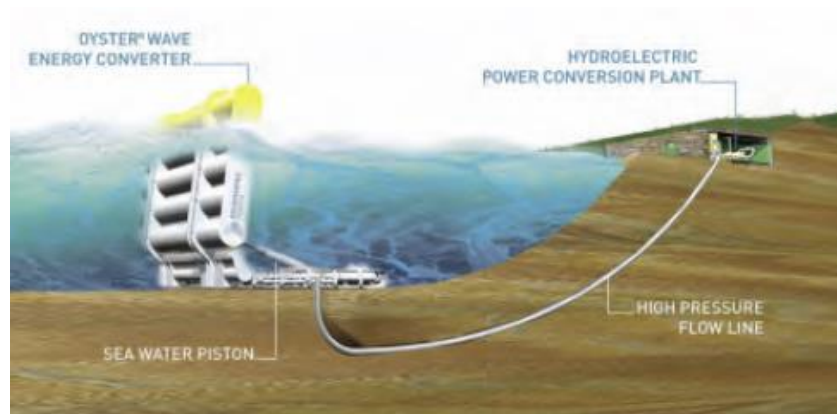


**Figure 35 An Oyster Wave Energy Converter Device (Flatley, 2009)**

Of course, Marine renewable energy and support for shipping/boating are only two sample applications that can benefit from the bathymetric data collection. As stated earlier, the ability to assess shorelines and shallow bathymetry for accurate nautical charts, characteristics of biological oceanography, impacts from climate change, beach erosion, sea level rise and many more subjects can benefit greatly from the capacities that bathymetric technologies currently provide and an even greater wealth as these technologies continue to grow and increase in capabilities.

## **5.2 Future Work**

At the time of this data collection there was discussion with the Army Geospatial Center Water Resources Group and they noted that for some shallow water data collection they were experimenting with towing a Sonar/Side-Scan Sonar fish behind a jet ski and collecting and processing that data. The Jet Ski collection data was not available for use at this time; however, it does open the door for additional data collection

techniques that have significantly cheaper collection methods, compared to flying or large vessels that decrease risk in collection, time to employ collection tools and overall costs to data collection methodologies. Also, additional calculations for verification and validation of mosaic and merge tools on the collected data would be follow on work to assess against ground truth and known bathymetric points to ensure the output product from the Mosaic tool.

With the development of CZMIL efforts and the work to improve on ABL collection capabilities, this technology should be reviewed in follow on research to assess the increase in technical capabilities that the CMIL effort brings to the bathymetry world in support of the vast array of applications discussed.

With respect to data merging, there are a multitude of methods in the literature to merge data. It is recommended that an additional assessment of those tools is made to verify and validate that the merging of data between different collection methods provides accurate data that can be used. Specific focus should be put on the analysis and discovery of the origin of the potential systematic difference identified with the Zonal Statistic analysis. If such analysis discovers that there are gaps in the capabilities to merge data, such as variations in z-values between data sets for identical geospatially referenced locations, additional research should be developed to address the gaps identified. On the other hand, if such research identifies a collection or processing change that can rectify identified issues, they can potentially be standardized for correction.

Follow-on research in this field, as well as in the recommended follow-on research points discussed above, in the next 5 years is anticipated to yield great advancements. It is with interest and a fundamental engineering desire to track this progress that this thesis is intended to incite with the desire to learn and gain knowledge as well as follow technologies in the fields that pose significant interest to the reader.

## REFERENCES

- Andritz. (2012). *Andritz Hydro Hammerfest*. Retrieved 2014 йил 8-August from <http://www.andritz.com/>: <http://www.andritz.com/hy-hammerfest.pdf>
- Applanix. (n.d.). Retrieved 2015, from [http://www.applanix.com/media/downloads/products/specs/POSAV\\_SPECS.pdf](http://www.applanix.com/media/downloads/products/specs/POSAV_SPECS.pdf)
- Bilaniuk, N., & Wong, G. S. (1993). Speed of sound in pure water as a function of temperature . *The Journal of the Acoustical Society of America* 93 , 1609-1612.
- Brock, S. J. (2009). The Emerging Role of LIDAR Remote Sensing in Coastal Research and Resource Management. *Journal of Coastal Research* , 1-5.
- Bukata, R. J. (1995). *Optical Properties and Remote Sensing of Inland and Coastal Waters*. CRC Press, Boca Raton,. Boca Raton: CRC Press.
- Calder, B. (2006). On the uncertainty of archive hydrographic datasets. *IEEE Journal of Oceanic Engineering* , 249-265.
- CARIS. (n.d.). Retrieved 2015, from <http://www.caris.com/products/hips-sips/>
- CIA. (2015). *The World Fact Book*. Retrieved 2015, from <https://www.cia.gov>: <https://www.cia.gov/library/publications/the-world-factbook/fields/2120.html>
- Clément, A. e. (2009). A review of wave energy converter technology. *Renewable & Sustainable Energy Reviews* , 405–431.
- Clement, A. e. (2002). Wave energy in Europe: current status and perspectives. *Renewable and Sustainable Energy Reviews Volume 6, Issue 5* , 405-431.
- Coleman, X. Y. (2011). Holes in the ocean: Filling voids in bathymetric lidar data. *Computers & Geosciences* , 474–484.
- Committee on National Needs for Coastal Mapping and Charting, M. S. (2004). *A Geospatial Framework for the Coastal Zone: National Needs for Coastal Mapping and Charting*. National Academies Press.



Costa, T. A. (2009). Comparative evaluation of airborne LiDAR and ship-based multibeam SoNAR bathymetry and intensity for mapping coral reef ecosystems. *Remote Sensing of Environment* , 1082–1100.

Crutchley, S. C. (2010). *The Light Fantastic: Using Airborne Lidar in Archaeological Survey*. Swindon: English Heritage Publishing.

Curcio, J. P. (1951). The near-infrared absorption spectrum of liquid water. *Journal of the Optical Society of America* , 302-304.

Davies-Colley, R. V. (1993). *Colour and Clarity of Natural Waters*. Ellis Horwood.

deSmith, M., Goodchild, M., & Longley, P. (2015). *Geospatial Analysis A Comprehensive Guide to Principles, Techniques, and Software Tools (Fifth Edition)*. Winchelsea: The Winchelsea Press.

Dodd, D., & Barbor, K. (2013). Coastal Zone Imaging and Mapping LIDAR Validation. *US Hydro* (pp. 1-19). New Orleans, Louisiana: Researchgate.

ESRI. (2015, July 27). Retrieved from <http://resources.arcgis.com/en/help/main/10.2/>

Finkl, C. B. (2005). Interpretation of seabed geomorphology based on spatial analysis of high-density airborne laser bathymetry. *Journal of Coastal Research* , 501-514.

Flatley, J. L. (2009, March 9). Oyster Wave Energy Converter puts climate change to good use. *Engadget* , p. 1.

Hackmann, W. D. (1986). Sonar Research and Naval Warfare 1914-1954: A Case Study of a Twentieth-Century. *Historical Studies in the Physical and Biological Sciences, Vol. 16, No. 1* , 83-110.

Hongxing Liu, K. C. (1999). Development of an Antarctic digital elevation model by integrating cartographic and remotely sensed data: A geographic information system based approach. *Journal of Geophysical Research, Vol. 104* , 199-213.

Hughes-Clarke, J. M. (1996). Shallow-water imaging multibeam sonars: A new tool for investigating sea floor processes in the coastal zone and on the continental shelf. *Marine Geophysical Researches* , 607-629.

Iampietro, P., Kvitec, R., & Erica, M. (2005). Recent Advances in Automated Genus-Specific Marine Habitat Mapping Enabled by High-End resolution Multibeam Bathymetry. *Marine Technology Society Journal, Volume 39 Number 3* , 83-93.

Irish, J. W. (1998). Coastal engineering applications of high-resolution LiDAR bathymetry. *Coastal Engineering* , 47-71.

- JALBTCX. (n.d.). Retrieved 2015, from <http://shoals.sam.usace.army.mil/>
- Jones. (1985). ASDIC to SONAR. *Nature (London)* , 201.
- Klein. (2015). Retrieved 2015, from <http://www.l-3mps.com/klein/pdfs/Klein-System-5000-V2-Sept-10.pdf>
- Klemas, V. (2011). Beach Profiling and LIDAR Bathymetry: An Overview with Case Studies. *Journal of Coastal Research* , 1019-1028.
- Kunath, M. A. (2011, November 28). State, Others Embrace New Roles in Global Shipping. *Ghanaian Chronicle* .
- Kvietk, R. e. (1999). *EARLY IMPLEMENTATION OF NEARSHORE ECOSYSTEM DATABASE PROJECT*. Seaside: VA Resource Center Institute for Earth Systems Science and Policy.
- L. Cameron, R. D. (2010). Design of the Next Generation of the Oyster Wave Energy Converter. *3rd International Conference on Ocean Energy* (pp. 1-11). Bilbao: Aquamarine Power Ltd.
- Lucian Drăgut, C. E. (2011). Object representations at multiple scales from digital elevation models. *Geomorphology* 129 , 183–189.
- Martin, J. D. (2014). 2014 National Economic Impact of the U.S. Coastal Port System. *American Association of Port Authorities' (AAPA) 2015 Spring Conference* (p. 5).
- District of Columbia: American Association of Port Authorities' (AAPA).
- Matsuyama, M. W. (1999). The effect of bathymetry on tsunami . *Geophysical Research Letters characteristics at Sisano Lagoon, Papua New Guinea* , 3513e3516.
- Meyer, B. (2015). You think those ships are big? *American Shipper*, Vol. 57(4) , 29.
- Newman. (1956). *The World of Mathematics Volume 1*. New York: Simon and Schuster.
- Nishida, T. M. (2001). Study of bathymetry effects on the nominal hooking rates of yellowfin tuna (*Thunnus albacares*) and bigeye tuna (*Thunnus obesus*) exploited by the Japanese tuna longline fisheries in the Indian Ocean. *Proceedings 4* (pp. 191-206). Indian Ocean Tuna Commission.
- NOAA. (n.d.). Retrieved 2015, from <http://www.noaa.gov/>

NOAA. (2014). *NOAA Office of Coast Survey*. Retrieved 2014, from [http://www.nauticalcharts.noaa.gov/hsd/hydro\\_history.html](http://www.nauticalcharts.noaa.gov/hsd/hydro_history.html)

NOAA. (2013). *NOAA.gov*. Retrieved from National Oceanic and Atmospheric Administration: <http://shoreline.noaa.gov/intro/timeline.html>

*NOAA Office of Coast Survey*. (2014). Retrieved 2014, from <http://www.nauticalcharts.noaa.gov/hsd/lidar.html>

Panicker, N. (1976). Power resource potential of ocean surface wave. *The Wave and Salinity Gradient Workshop*, (pp. 1-48). Newark.

Purkis, S. a. (2011). *Remote Sensing and Global Environmental Change*. Oxford, U.K.: Wiley-Blackwell.

Ram, K. e. (2014). In situ near-shore wave resource assessment in the Fiji Islands. *Energy for Sustainable Development* (23) , 170-178.

Ring, J. (1963). The Laser in Astronomy. *New Scientist* , 672-673.

Saylam, K. (2009). QUALITY ASSURANCE OF LIDAR SYSTEMS –MISSION PLANNING. *ASPRS 2009 Annual Conference* (pp. 1-13). Baltimore, Maryland: GeoBC Crown Registry and Geographic Base (CRGB) Branch.

Sea-Bird, E. (n.d.). Retrieved 2015, from [http://ftp.seabird.com/products/spec\\_sheets/19plusdata.htm](http://ftp.seabird.com/products/spec_sheets/19plusdata.htm)

Simon P. Neill, M. R. (2013). Wave power variability over the northwest European shelf seas. *Applied Energy Volume 106* , 31-46.

TRITON. (n.d.). Retrieved 2015, from <http://www.tritonimaginginc.com/site/content/software/suites/index.htm>

USGS. (n.d.). Retrieved 2015, from <http://www.usgs.gov/>

USGS. (2014, November 24). *WHSC Bathymetry systems*. Retrieved July 7, 2015, from <http://woodshole.er.usgs.gov>:  
<http://woodshole.er.usgs.gov/operations/sfmapping/swath.htm>

Wang, W. D. (2007). Using Airborn Bathymetric Lidar to Detect Bottom Type Variation in Shallow Waters. *Science Direct* , 123-135.

Wozencraft, J. a. (2003). SHOALS Airborne Coastal Mapping: Past, Present, and Future. *Journal of Coastal Research* , 207-215.

Zhang, T., & Ge, L. (2007). A decomposition of Moran's I for clustering detection. *Computational Statistics & Data Analysis* 51 , 6123 – 6137.

## **BIOGRAPHY**

Prior to joining the Army Geospatial Center (AGC), Geoffrey S. Cleveland was a General Engineer for Space and Naval Warfare Systems Command (SPAWAR) responsible for coordinating external, independent reviews for program Systems Engineering Technical Review (SETR) events as the SPAWAR 5.0 Technical Authority (TA) for Business IT as well as providing systems engineering technical support to Program Executive Office (PEO) Enterprise Information Systems (EIS) programs. Before SPAWAR, Mr. Cleveland was a General Engineer for Marine Corps Systems Command (MCSC) in Quantico, VA responsible for systems engineering across MCSC product groups. Before MCSC, Mr. Cleveland was an Integrated Product Team (IPT) Lead for the Direct Reporting Program Manager (DRPM), U.S. Marine Corp in Woodbridge, VA responsible for communication, navigation, EMI efforts for the Expeditionary Fighting Vehicle (EFV). Before the MCSC IPT Lead position, Mr. Cleveland worked at General Dynamics where he was a Senior Electrical Engineer and Manager for the Electrical Power Management IPT on the DRPM EFV program. Mr. Cleveland began his working career at Assurance Technology Corp., where he was an Electrical Engineer working on hardware and software programs.

Mr. Cleveland earned a Bachelor of Science in Electrical Engineering from North Carolina State University, is finalizing his thesis for a M.S. in Geospatial Engineering and has level III certification in System Planning, Research, Development and Engineering – System Engineering, level III certification in Program Management, and level I certification in Test & Evaluation from the Defense Acquisition University. Mr. Cleveland was on active duty in the U.S. Marine Corp for four years as an Amphibious Assault Vehicle (AAV) repairman and spent 3 years in the Marine Corps Reserves where he was cross trained in Logistics.